

# A review on GaN HEMTs: nonlinear mechanisms and improvement methods

**Chenglin Du<sup>1,2</sup>, Ran Ye<sup>1,2,†</sup>, Xiaolong Cai<sup>1,2,†</sup>, Xiangyang Duan<sup>1,2</sup>, Haijun Liu<sup>2</sup>, Yu Zhang<sup>2</sup>, Gang Qiu<sup>2</sup>, and Minhan Mi<sup>3</sup>**

<sup>1</sup>State Key Laboratory of Mobile Network and Mobile Multimedia Technology, Shenzhen 518055, China

<sup>2</sup>Wireless Product Planning Department, ZTE Corporation, Shenzhen 518055, China

<sup>3</sup>School of Microelectronics, Xidian University, Xi'an 710071, China

**Abstract:** The GaN HEMT is a potential candidate for RF applications due to the high frequency and large power handling capability. To ensure the quality of the communication signal, linearity is a key parameter during the system design. However, the GaN HEMT usually suffers from the nonlinearity problems induced by the nonlinear parasitic capacitance, transconductance, channel transconductance etc. Among them, the transconductance reduction is the main contributor for the nonlinearity and is mostly attributed to the scattering effect, the increasing resistance of access region, the self-heating effect and the trapping effects. Based on the mechanisms, device-level improvement methods of transconductance including the trapping suppression, the nanowire channel, the graded channel, the double channel, the transconductance compensation and the new material structures have been proposed recently. The features of each method are reviewed and compared to provide an overview perspective on the linearity of the GaN HEMT at the device level.

**Key words:** GaN HEMT; linearity improvement; transconductance reduction; transconductance compensation; nanowire channel; graded channel

**Citation:** C L Du, R Ye, X L Cai, X Y Duan, H J Liu, Y Zhang, G Qiu, and M H Mi, A review on GaN HEMTs: nonlinear mechanisms and improvement methods[J]. *J. Semicond.*, 2023, 44(12), 121801. <https://doi.org/10.1088/1674-4926/44/12/121801>

## 1. Introduction

Gallium nitride (GaN) is regarded as an extremely potential material for high power applications due to its wide band gap and high breakdown field<sup>[1–3]</sup>. A high electron mobility transistor (HEMT) is popular for high-frequency applications because of its high-density two dimensional electron gas (2DEG) originated from the GaN-based hetero-junction<sup>[4–7]</sup>. With the development of the wireless communication system, the network needs to offer a greater data transfer rate, lower transmission delay and higher signal quality, which requires high-performance electronic devices<sup>[8, 9]</sup>. Nowadays, more and more GaN HEMTs are employed into radio frequency (RF) front ends to replace conventional silicon-based devices due to their excellent properties<sup>[10–12]</sup>.

In the RF front ends, to ensure the quality of communication, linearity is a key parameter in system design. Nonlinearity problems result in significant side bands, saturation of output power at high input powers, an increase of error vector magnitude and further deteriorates the transmission quality of signal<sup>[13–15]</sup>. Thus, many circuit-level methods have been proposed to overcome this nonlinearity problem including the back-off, the feed-forward, the feedback, the digital pre-distortion, etc.<sup>[16–21]</sup>. However, as the operation frequency increases gradually to cater to high data capacity, the imple-

mentation of circuit-level linearization turns out to be more and more complex and high-cost. As a core device in the RF front ends, a direct improvement of linearity upon the GaN HEMT is one of effective and low-cost methods to suppress the nonlinearity problem in the system.

Over the past decade, the GaN HEMT was widely applied in the commercial wireless communication field due to its superior performance<sup>[22–24]</sup>. With the massive deployment of the GaN HEMT, the linearity issue attracts more and more attention. Plenty of investigations on the device linearity improvement for the GaN HEMT have emerged for more competitive device performances, such as modification, optimization or innovation of the device structure and fabrication process. In order to provide an overview perspective on the GaN HEMT that serves as references for high linearity and high-performance devices in the future, in this review, we summarize the main nonlinear sources in the GaN HEMT. Then, the physical mechanisms of nonlinearity, especially transconductance, at the device level are discussed and analyzed for the GaN HEMTs. At the end, according to these mechanisms, many device-level improvement methods in recent years are reviewed and discussed.

## 2. Nonlinear sources of GaN HEMTs

The fifth-generation (5G) wireless communication system needs high signal transmission quality to satisfy the low transmission delay. In practical system applications, if the linearity of the power amplifier (PA) is poor, the signal is susceptible to interference from adjacent channels, resulting in a high bit error rate. The system has to transmit the signal sev-

Correspondence to: R Ye, [ye.ran@zte.com.cn](mailto:ye.ran@zte.com.cn); X L Cai, [cai.xiaolong@zte.com.cn](mailto:cai.xiaolong@zte.com.cn)

Received 13 APRIL 2023; Revised 31 MAY 2023.

©2023 Chinese Institute of Electronics

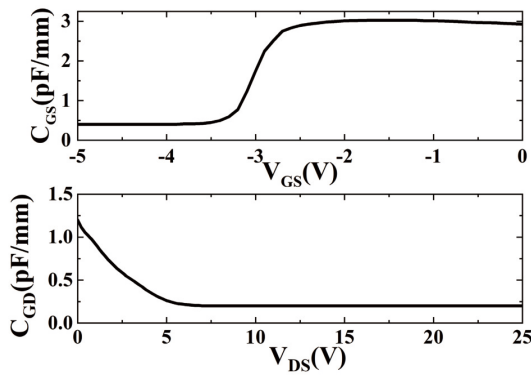


Fig. 1. Relationship between capacitance and voltage for GaN HEMT.

eral times to improve communication quality and then the transmission delay increases. Thus, it requires very stringent linearity for PAs in the RF front ends<sup>[25]</sup>. The nonlinearity of PAs is usually characterized by the intermodulation distortion (IMD), the amplitude modulation to amplitude modulation (AM/AM) distortion and the amplitude modulation to phase modulation (AM/PM) distortion.

One obvious property of a nonlinear system is its harmonics generation of the excitation frequency or frequencies. The intermodulation products are mixture components with different frequencies generated from nonlinear device elements. When two input signals with  $\omega_1$  and  $\omega_2$  are applied to the input terminal of the PA, besides the fundamental signal at a  $\omega_1$  and  $\omega_2$ , the output signal also contains many mixed harmonics due to the nonlinear effect. Because the third-order intermodulation (IMD3) products at  $2\omega_1-\omega_2$  and  $2\omega_2-\omega_1$  are close to the fundamental frequency and difficult to filter, usually, the IMD3 attracts more attention than others.

The AM/AM distortion is a nonlinear power relationship between input signal and output signal. With the input power increasing, the output power no longer increases linearly. As a result, the AM to AM conversion is not kept as a constant. Similarly, the AM/PM distortion is a phenomenon wherein changes in the amplitude of a signal applied to a nonlinear circuit cause a phase shift. This distortion can lead to serious consequences if it occurs in a system in which the signal's phase is important.

Based on the Volterra Series analysis, the nonlinearity mainly comes from the transconductance ( $g_m$ ), the channel transconductance ( $g_{DS}$ ), the gate-to-source capacitance ( $C_{GS}$ ) and the gate-to-drain capacitance ( $C_{GD}$ )<sup>[26, 27]</sup>. The top picture of Fig. 1 shows the nonlinear variation of  $C_{GS}$  versus gate-to-source voltage ( $V_{GS}$ ). Due to the existence of 2DEG,  $C_{GS}$  decreases rapidly near the pinch-off voltage. Likewise, the variation of  $C_{GD}$  versus the drain-to-source voltage ( $V_{DS}$ ) is displayed in the bottom picture of Fig. 1 and it is also nonlinear with  $V_{DS}$ . Owing to these variations, the capacitances have nonlinear impacts on the linearity of RF PAs. It is reported that a growing significance of  $C_{GS}$  induced the IMD role when the frequency increases in the microwave region and certain bias shifts of the mentioned sweet spot<sup>[28]</sup>. According to the expression of physical model analyzed in Ref. [13], both  $C_{GS}$  and  $C_{GD}$  can lead to the AM/AM and AM/PM distortion. Especially in the GaN based PAs, the AM/PM distortion is contributed by the input impedance variation due to the nonlinear  $C_{GS}$  and  $C_{GD}$ <sup>[29]</sup>.

Fig. 2 shows the  $g_m$  and  $g_{DS}$  curves as the function of  $V_{GS}$  and  $V_{DS}$ , respectively. In a certain range of  $V_{GS}$  and  $V_{DS}$ , the values of  $g_m$  and  $g_{DS}$  change nonlinearly. However, the nonlinear change of  $g_m$  is worse and the linear region of  $g_m$  is narrower. According to Eqs. (1) and (2), the harmonics  $v_{O2}$  and  $v_{O3}$  are proportional to the first derivative of  $g_m$  ( $g'_m$ ) and the second derivative of  $g_m$  ( $g''_m$ )<sup>[30]</sup>. The output third-order intercept power (OIP3) is related to the  $g_m$  and  $g''_m$  according to Eq. (3)<sup>[31]</sup>.

$$v_{O2} \propto \frac{g'_m A^2 (1 + \cos(2wt))}{2}, \quad (1)$$

$$v_{O3} \propto \frac{g''_m A^3 (3\cos(\omega t) + \cos(3\omega t))}{4}, \quad (2)$$

$$\text{OIP3} = 10\log_{10} \left( \frac{2g'_m}{3g''_m} R_{\text{Load}} \right) + 30. \quad (3)$$

Except for the above sources, the bias condition, the source/load impedance, the operation frequency, the gate leakage current, the drain-to-source capacitance are possible to lead to the nonlinearity of the GaN HEMT<sup>[31–33]</sup>. However, as for the GaN HEMT, the parasitic capacitance is usually small and the other nonlinear effects are relatively not obvious. Generally, the transconductance ( $g_m$ ) is considered as the most main nonlinearity contributor in the GaN HEMT<sup>[31, 32]</sup>. Therefore, we mainly focus on the physical mechanism of the nonlinear  $g_m$  for the GaN HEMT in detail.

### 3. Physical mechanisms of nonlinear transconductance

To conveniently describe the  $g_m$  profile or the  $g_m$  flatness, a gate voltage swing (GVS), which is a gate voltage range that has at least its 80% peak  $g_m$  value, is defined as a figure of merit to indicate the linearity at the device level<sup>[34]</sup>. In this way, if the wider GVS is, the lower values of  $g'_m$  and  $g''_m$  will be, meaning that the harmonic outputs are suppressed. In order to achieve the wider GVS, the physical mechanisms of that  $g_m$  reduced with the gate voltage are discussed in many works.

#### 3.1. Scattering effect

The sheet concentration of 2DEG  $n_s$  is changed by the gate easily because the 2DEG is distributed in a narrow range of the hetero-interface. As the gate voltage increases, the electron concentration rises rapidly and the electron mobility and velocity reduces due to the scattering effect. The longitudinal optical phonon is found to be responsible for the electron velocity reduction, further causing the drift velocity to saturate, particularly in the place where high sheet carrier densities exist due to the hot phonon effect<sup>[35, 36]</sup>. Fang *et al.*<sup>[37]</sup> also took the effect of optical phonon scattering on the electron velocity into consideration. It is demonstrated that the saturation current is proportional to  $\sqrt{n_s}$  at high carrier concentration, and the  $g_m$  will decrease as  $g_m \sim 1/\sqrt{n_s}$ . Bajaj *et al.*<sup>[38]</sup> successfully calibrated the transport model, including the effect of optical phonon scattering on electron velocity by the direct sheet density measurement.

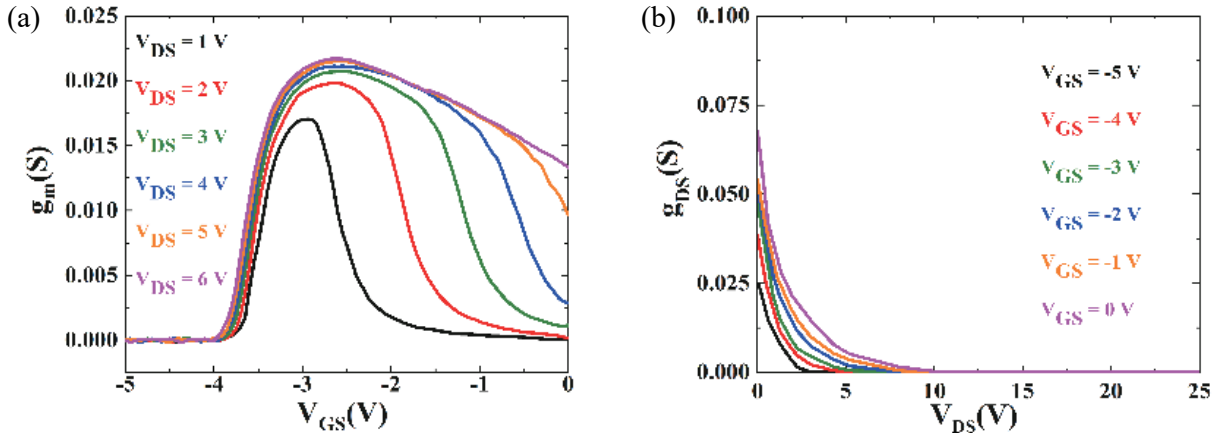


Fig. 2. (Color online) GaN HEMT: (a) transconductance  $g_m(V_{GS})$  curves. (b) Channel transconductance  $g_{DS}(V_{DS})$  curves.

In addition, the interface roughness scattering is responsible for the reduction of the electron mobility and velocity. Juang *et al.*<sup>[39]</sup> reported that the electron wave function is pressed closely against the AlGaN/GaN hetero-interface in the high electron concentration state, which causes the electron mobility to drop off due to the interface roughness scattering. Especially, the effect of interface roughness scattering is more serious with the high gate voltage that induces the high electron concentration. Li *et al.*<sup>[40]</sup> demonstrated that the high perpendicular electric field generated by gate voltage aggravates the interface roughness scattering and degrades the electron velocity. With the increasing gate voltage, the electron velocity begins to reduce. This is expected since the changes of the gate voltage primarily affect the interface scattering while the other processes are only mildly changed.

### 3.2. Access resistance

To ensure the high-power handling capability, the source and drain regions of GaN HEMT are not self-aligned with the gate electrode. However, the non-self-aligned structure brings in extra parasitic access resistance in the source and drain regions, as shown in Fig. 3. Palacios *et al.*<sup>[41]</sup> demonstrated that the increasing of dynamic source access resistance ( $r_s$ ) is the main reason for the  $g_m$  reduction. With the increasing gate voltage, the electric field is higher than 10 kV/cm. At this electric field, the electron velocity has already started its “quasi-saturation” which produces a decrease in the electron mobility, along with the increasing  $r_s$  (see Fig. 4)<sup>[42, 43]</sup>.

Trew *et al.*<sup>[44]</sup> reported that the increasing  $r_s$  is attributed to the space charge limitation under the high current state. Under this condition, the injected charges in the semiconductor become comparable in magnitude to the background impurity density when the device stays under large-signal RF operation. Once space charge limitation is established, the resistivity increases rapidly with the current and the distance from the source injection point. In this way, the  $r_s$  expression is formed in Eq. (4), where  $r_{ss}$  denotes the low current magnitude of the resistance in the gate–source region,  $\Delta r_{ss}$  denotes the increased resistance due to the space charge limitation,  $I_{sc}$  denotes the space charge threshold current. Except for the space charge limitation effect, the polarization coulomb field (PCF) scattering is discussed as one reason for the increasing  $r_s$  with a longer gate length or a shorter gate-

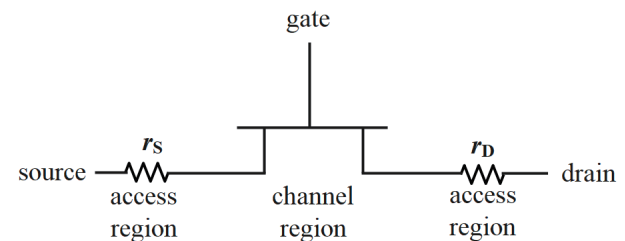


Fig. 3. Parasitic source and drain access resistances of GaN HEMT.

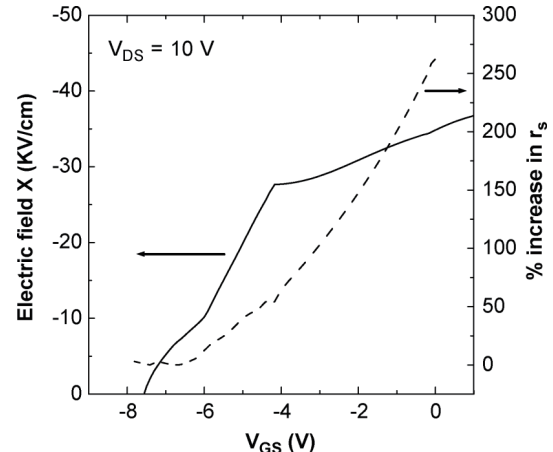


Fig. 4. Longitudinal electric field at the source access region for different  $V_{GS}$ . The simulated increase in  $r_s$  is plotted in the right axis<sup>[41]</sup>.

source distance by Yang *et al.*<sup>[45]</sup>.

$$r_s = r_{ss} + \Delta r_{ss} = \frac{r_{ss}}{1 - \frac{I}{I_{sc}}} \quad (4)$$

The drain access resistance ( $r_D$ ) is also taken into account for the  $g_m$  reduction according to Chen *et al.*<sup>[46]</sup>. The high  $r_D$  pushes the device from the saturation state to the linear state, which causes the  $g_m$  reduction. Considering the gate-controlled voltage is closely related to the value of  $r_s$ , the dynamic change of  $r_s$  attracts more attention according to the reported studies. However, the dynamic change of  $r_D$  also needs attention due to its negative effect.

### 3.3. Self-heating effect

The self-heating effect is common in the Si device when it operates at a high power state. In the GaN HEMT, the self-

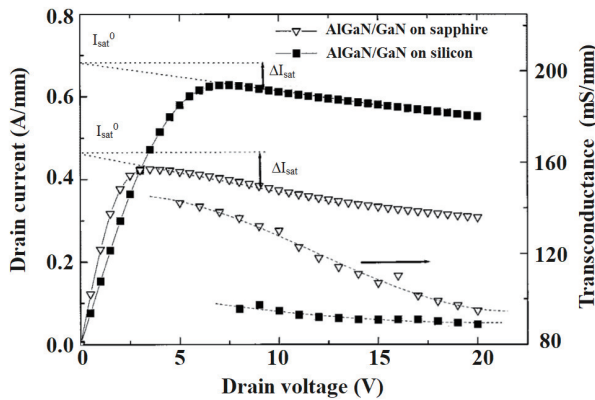


Fig. 5. AlGaN/GaN HEMT output and transconductance characteristics at  $V_{GS} = 0$  V<sup>[47]</sup>.

heating effect on  $g_m$  is investigated by Kuzmik *et al.*<sup>[47]</sup>. As expected with Si, if the device temperature is raised, the low-field electron mobility in the channel decreases, and the channel resistance related to the  $r_s$  increases. As a result, the  $g_m$  and drain saturation current ( $I_{sat}$ ) are dispersed with the increasing drain voltage. It is noted that, in Fig. 5, the  $g_m$  dispersion of the sapphire substrate with worse heat dissipation rate is more steep. The  $\Delta I_{sat}$  is defined as a difference  $I_{sat} - I_{sat}^0$ , where  $I_{sat}$  is a value in a particular HEMT working point and  $I_{sat}^0$  denounces a reference value of the channel at room temperature ( $I_{sat}^0$  is obtained by extrapolating  $I_{sat}$  to  $V_{DS} = 0$  V). Chen *et al.*<sup>[46]</sup> further discussed that, with the increasing drain voltage and gate voltage, the transfer and  $g_m$  curves are easier to be pushed into the region affected by the self-heating, and then they begin to decrease.

#### 3.4. Trapping effects

Due to the tough growth of GaN-based material, such as dislocations, dangling bonds, vacancies are inevitably brought in the GaN HEMT, which will become the latent sources of traps. The influences of trapping effects on the GaN HEMT usually present as the gate-lag, the drain-lag, the current collapse, the frequency dispersion etc.<sup>[48–53]</sup>. Specifically, the gate-lag and the drain-lag are transient responses of the drain current under the transient stress<sup>[54]</sup>. During the stress period, electrons are captured by traps and they have not enough time to de-trap after the stress period due to the long time constant. In this way, the drain current is lower than normal and gradually recovers with time. The current collapse is measured under the condition that the gate and drain are pulsed from the quiescent bias point ( $V_{GS,Q}$  &  $V_{DS,Q}$ ), usually based on the practical operation state, to a voltage respectively. On account of the gate-lag and the drain-lag, the drain current of  $I_{DS}-V_{DS}$  characteristic turns to collapse and slump accordingly. As shown in Fig. 6, the  $g_m$  reduces obviously with different quiescent bias points under the pulse measurement. Besides, a threshold voltage drift towards the positive voltage direction is also observed, which is mainly affected by the gate quiescent bias stress. This effect indicates that traps are present at the interface between the gate and the AlGaN layer, and can effectively change the threshold voltage. Therefore, once these traps are charged by a negative gate voltage pulse, a shift of the  $g_m$  curve with respect to the (0 V, 0 V) bias point is obtained<sup>[55]</sup>.

For the GaN HEMT, the traps were reported in the AlGaN

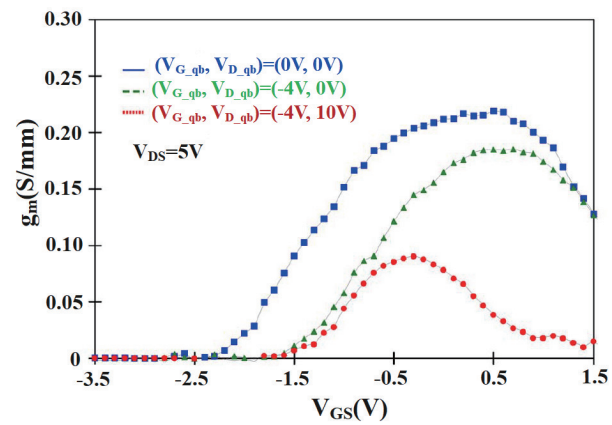


Fig. 6. (Color online) Pulsed  $g_m$  versus  $V_{GS}$  characteristics for the GaN HEMT with different quiescent bias point<sup>[55]</sup>.

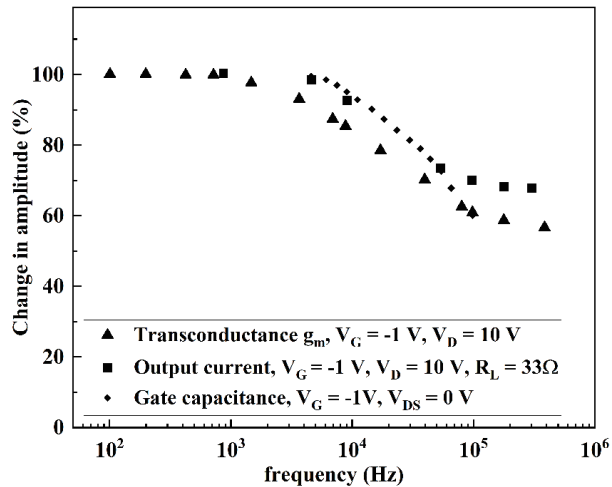


Fig. 7. Frequency dispersion of output current, transconductance at quiescent large signal bias point, and gate capacitance at  $V_{DS} = 0$  V<sup>[61]</sup>.

barrier, the AlGaN surface and the GaN buffer. The trapping behaviors usually occur in the region with a high electric field, typically in the gate-drain access region<sup>[56, 57]</sup>. Meneghesso *et al.*<sup>[58]</sup> demonstrated that when a high drain-gate bias is applied to the device, electrons may tunnel from the gate toward surface states located within the gate-drain access region: The accumulation of negative charge acts as a virtual gate at the surface of the HEMT, and induces an increase of the channel resistance, and a decrease of the peak  $g_m$ . Du *et al.*<sup>[59]</sup> found that the acceptor-like traps in the barrier layer under the gate is the main cause of nonlinear  $g_m$  behavior. When a high drain voltage applied on the device which is doped with C/Fe to improve resistivity, the traps in the buffer capture the electrons in the 2DEG and induce a serious drain current collapse, further causing the  $g_m$  reduction<sup>[55, 60]</sup>. Furthermore, due to the different time constant of the traps, the frequency response is not alike. Kohn *et al.*<sup>[61]</sup> reported that, with the increasing frequency of the transconductance, the gate capacitance and the output current of the GaN HEMT, a compression tendency exists (see Fig. 7). Based on the results, it can be demonstrated that the trapping effects are the reasons for the  $g_m$  nonlinearity.

According to the discussions above, there are three main causes that reduce  $g_m$  in the channel region, including the scattering effect, the self-heating effect and the trapping effects.

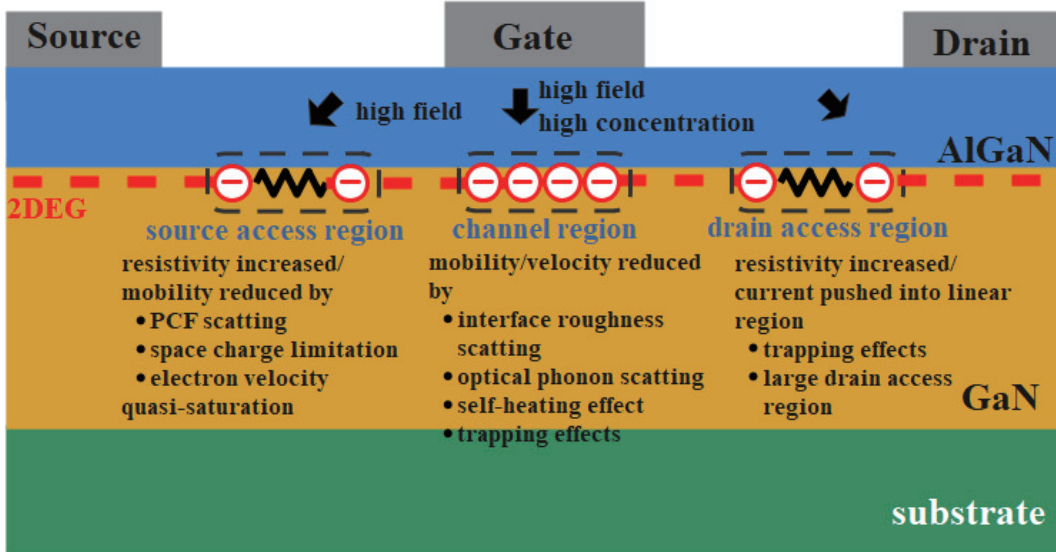


Fig. 8. (Color online) Existing mechanisms of  $g_m$  reduction for the GaN HEMT.

Due to the scattering effect, the high electric field and the high electron concentration induced by the increasing gate voltage reduce the electron velocity or mobility. As for the self-heating effect, the electron mobility is decreased with the increasing channel temperature and  $g_m$  reduces as a result. With the change of the gate voltage, the traps under the gate trap or de-trap the electrons and increase the channel resistivity when trapping effects begin to work.

Except for the intrinsic  $g_m$  of the GaN HEMT, the effect of the access region on the  $g_m$  reduction is attributed to the other causes. The increasing  $r_s$  results from the electron mobility reduction induced by high electric field, the electron mobility reduction induced by PCF scattering and the resistivity rise induced by the space charge limitation. In the drain access region, the trapping is one reason for the resistivity increase due to the large electric field. The increasing  $r_D$  has also an impact on the  $g_m$  reduction. Usually, to deal with higher voltage, the device is equipped with the large drain access region that increases  $r_D$ . If  $r_D$  is large, the operation state of the GaN HEMT will be pushed easier into linear region with the increasing gate voltage and  $g_m$  reduces as a consequence. The mechanisms of nonlinear  $g_m$  are reviewed in Fig. 8 to show an overview for the different regions in the GaN HEMT.

#### 4. Improvement methods of transconductance

Differing from the circuit-level linearization techniques, the improvement at the device level has more benefits, such as the low complexity, the low cost and the easy realization. In light of the aforementioned problems, plenty of device-level methods were proposed to suppress the nonlinear problems.

The improvement methods for the nonlinear capacitance are relatively few. For example, Xue *et al.*<sup>[62]</sup> added a gate diode to compensate the nonlinear  $C_{GS}$  for the GaN HEMT. Bothe *et al.*<sup>[63]</sup> designed a new sunken source field plate to reduce  $C_{GS}$  and  $C_{GD}$  by 15% and 60% respectively. More device-level methods concentrate on the improvements of  $g_m$  flatness to achieve a large GVS. Previously, many simple methods were proposed to improve the  $g_m$  flatness, such as the field plate reducing the channel electric field<sup>[64]</sup>,

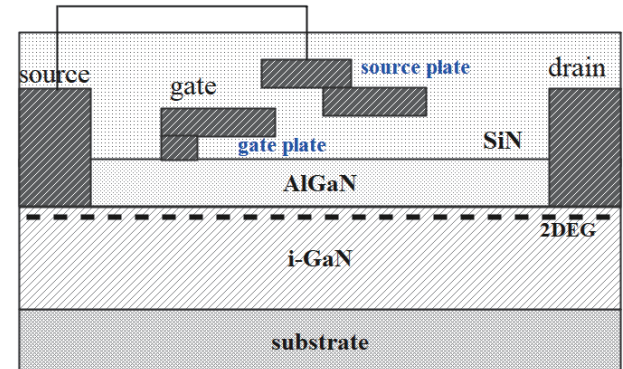


Fig. 9. (Color online) Schematic diagram of gate and source field plate of GaN HEMT.

the self-aligned source and drain eliminating the access resistance<sup>[65, 66]</sup>, the optimization of some structure parameters<sup>[67, 68]</sup>. However, the effect of these methods seems to be not satisfied with the current requirements. Recently, many novel device-level methods surged to achieve better effects.

##### 4.1. Suppression of trapping effects

As one main source of  $g_m$  reduction, the suppression methods of the trapping effects are discussed first. According to the trap positions, plenty of effective methods of suppressing the trapping effects were proposed. The application of the gate/source field plate reduces the surface electric field and further decreases the electron tunneling possibility through the gate. As a result, gate/source field plate is useful to reduce the trapping risk from the surface traps in the drain access region (see Fig. 9)<sup>[57, 69-71]</sup>.

Surface passivation is a method that directly eliminates the surface dangling bonds and improves the surface chemical stability, which reduces the density of surface traps. The  $\text{SiN}_x$  deposited by metal-organic chemical vapor deposition (MOCVD), or plasma-enhanced chemical vapor deposition (PECVD) is one of the most used passivation materials<sup>[72-74]</sup>. Although many novel passivation materials were still reported to obtain better performance, such as  $\text{MgO}$ ,  $\text{ScO}_3$ ,  $\text{Al}_2\text{O}_3$ ,  $\text{AlN}$ ,  $\text{MgF}_2$ , and  $\text{TiO}_2$ <sup>[75-80]</sup>. However, the passivation deposition process is negative for the device features, such

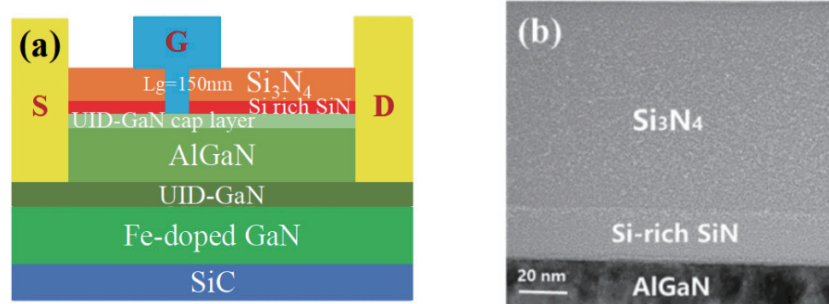


Fig. 10. (Color online) (a) Cross section of AlGaN/GaN HEMTs with Si-rich SiN interlayer. (b) TEM of devices with Si-rich SiN interlayer<sup>[84]</sup>.

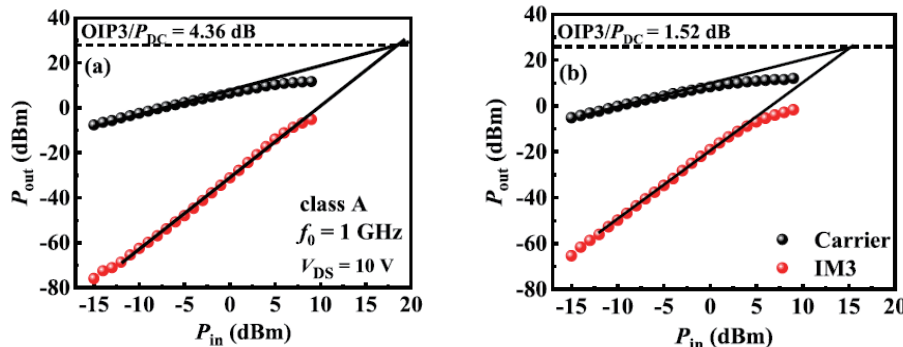


Fig. 11. (Color online) Two-tone linearity measurement at 1 GHz with a 1-MHz spacing of the (a) proposed device and (b) conventional device. Devices are biased at  $V_{DS} = 10$  V near class A<sup>[85]</sup>.

as the degradation of the leakage current, the breakdown voltage and the high-frequency characteristics<sup>[81–83]</sup>. Recently, multi-layer passivation became a new method to handle these problems. Liu *et al.*<sup>[84]</sup> developed a bilayer Si-rich SiN/Si<sub>3</sub>N<sub>4</sub> passivation which has the ability to reduce the gate leakage current and suppressing current collapse (see Fig. 10). Jing *et al.*<sup>[85]</sup> proposed a hybrid PECVD-SiN<sub>x</sub>/PECVD-SiO<sub>2</sub> passivation layer for the GaN HEMT. The SiO<sub>2</sub> is used to suppressing the surface traps in the drain access while the SiN<sub>x</sub> is used to modulate the charge and electric field in the source access region. As seen in the results in Fig. 11, besides the suppression of trapping effects, a 2.84 dB improvement of OIP3/P<sub>DC</sub> is obtained due to the PECVD-SiN<sub>x</sub> in the source access region when compared to the conventional one.

Except for the surface passivation, a GaN cap layer is another method to reduce the surface traps. The thin GaN layer is considered to compensate the negative polarization charge or to protect the 2DEG from the surface states<sup>[86–89]</sup>. The traps in the buffer are more difficult to directly eliminate during the device fabrication because the buffer is sandwiched between the substrate and the barrier layers. In consideration of the source of buffer traps, it requires a sophisticated control of native defects and unintentional dopants during the epitaxy of material<sup>[90]</sup>. Meanwhile, several novel epitaxial structures were proposed. A buffer-free structure is proposed to suppress the buffer-induced trapping effects. Compared with the conventional Fe-doped buffer, the structure allows for a thin 250 nm-thick unintentional doped GaN layer grown between an AlGaN barrier layer and an AlN nucleation layer<sup>[91]</sup>. Yao *et al.*<sup>[92]</sup> demonstrated that, by inserting a graded AlGaN back-barrier between the GaN channel and the AlGaN buffer layer, the trapping in the buffer induced by the

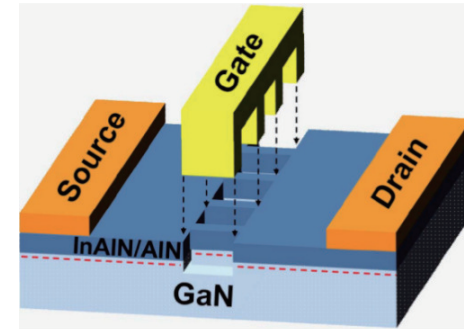


Fig. 12. (Color online) Device structure of nanowire channel HEMT<sup>[95]</sup>.

hot-electron effect is effectively blocked, which contributes to a remarkable suppression of the current collapse in the GaN HEMT. It is well known that the growth quality of the GaN buffer is better in the homo-epitaxial GaN substrate. Then, a GaN-on-GaN substrate with an acceptable cost was proposed recently<sup>[93]</sup>. In a word, the trapping effects are hot and complex issues in the GaN HEMT. Except for the above-mentioned suppression methods, other diverse methods are summarized in our previous work in detail<sup>[94]</sup>.

Although, the  $g_m$  reduction induced by the trapping effects is suppressed by the aforementioned methods. However, the  $g_m$  flatness cannot be improved further. Therefore, several novel methods for improving the GVS are introduced as follows.

#### 4.2. Nanowire channel

According to the above-mentioned mechanisms, the increasing  $r_s$  is considered as one reason for the  $g_m$  roll-off. Lee *et al.*<sup>[95]</sup> proposed a kind of nanowire channel HEMT structure aiming to suppress the increase of  $r_s$ . As shown in Fig. 12, the channel is surrounded with a gate electrode,

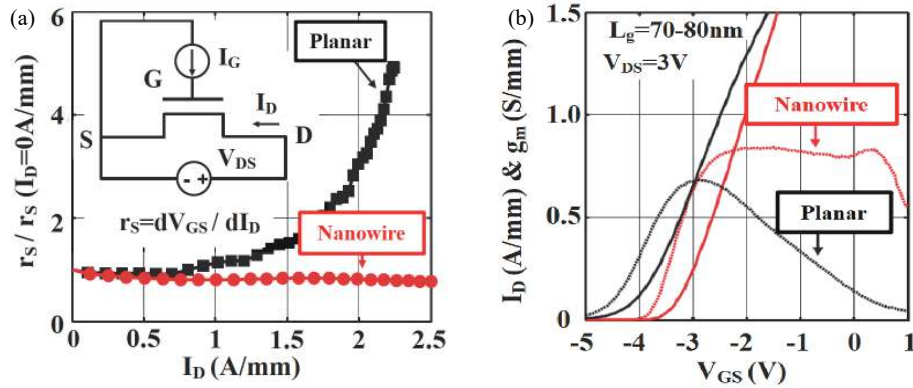


Fig. 13. (Color online) (a) Source resistance as a function of drain current density in planar and nanowire devices. Inset: measurement setup. (b) Transfer characteristics of nanowire channel and planar device<sup>[95]</sup>.

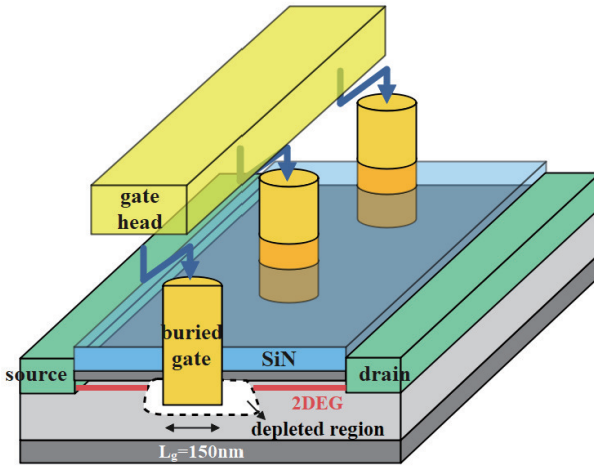


Fig. 14. (Color online) Schematic illustration of a GaN field-effect transistor with buried dual gates<sup>[101]</sup>.

which bears a close resemblance to the silicon-based fin field-effect transistor (FET)<sup>[96]</sup>, so it is also called as Fin-HEMT or tri-gate HEMT device<sup>[97, 98]</sup>. Fig. 13(a) displays the measured results of  $r_s$  for nanowire channel HEMT and planar HEMT. Obviously, the  $r_s$  of the nanowire channel HEMT is totally suppressed when compared with the planar one because of the relatively larger current drivability of its source access region. Namely, the source access region is larger than the channel region, which has more current handling ability to reduce the risk of space charge limitation. The  $g_m$  is flatter than that of planar HEMT as a result, as seen in Fig. 13(b).

In the following years, the nanowire channel HEMT structure was continuously investigated and discussed. The influence of fin configuration was investigated in detail by Zhang *et al.*<sup>[99]</sup> and they found that the threshold voltage is dependent with the width and height of fin. The  $g_m$  flatness is sensitive to the length and height of fin because of the modulation of  $r_s$  and sidewall-controlled gate capacitance. Based on the nanowire channel structure, Zhang *et al.*<sup>[100]</sup> proposed a Fin-HEMT with T-shaped gate which equipped with extreme flatness of extrinsic  $g_m$ . The proposed device offers an obvious improvement of 5.5 dBc in IMD3 distortion at high input power level. Shinohara *et al.*<sup>[101]</sup> proposed a GaN HEMT with buried dual gates depicted in Fig. 14, where parallel cylindrical gates were buried into an epitaxial structure by using

plasma dry etch. With the benefit of the cylindrical gates, the value of  $r_s$  is reduced effectively due to its wider ohmic contact width than other Fin-HEMTs. Odabasi *et al.*<sup>[102]</sup> also proposed a laterally gated HEMT device with high linearity performance (see Fig. 15(a)). It is illustrated that the previous cylindrical gates are replaced by the cubic gates. By optimizing the width of channel that remains between the combs of the gate metal and the width of metals that penetrates into the substrate, nearly constant  $g_m$  over a wider gate voltage range and a value of 31.7 dBm in OIP3 at 3.5 GHz are reached (see Fig. 15(b)). Even so, the fin structure has its own limitations. For example, the nanowire channel sacrifices parts of channel and decreases the output drain current. The multi-gate of fin structure brings in the extra parasitic gate capacitance that aggravates the frequency characteristic.

Aiming to break these limitations and obtain higher device performance, a super-lattice castellated FET was fabricated on an AlGaN/GaN super-lattice with six stacked heterostructures by Chang *et al.*<sup>[103]</sup> (see Fig. 16(a)). By virtue of its parallel 2DEG channel, a lower knee voltage and a higher output current ( $I_{DS} > 1.8 \text{ A/mm}$ ,  $P_{out} > 6 \text{ W/mm}$ ) are realized. Not only the superior  $I_{DS}-V_{DS}$  characteristics, the device also provides a high  $g_m$  over a wider gate voltage range due to the fin-like structure, and an OIP3/P<sub>DC</sub> of 6 dB at 30 GHz is realized (see Fig. 16(b)). Shinohara *et al.*<sup>[104]</sup> proposed buried dual-gate FETs based on the buried dual gate and 4-channel epitaxial structure to increase the drain current density and maintain the high linearity simultaneously. Xing *et al.*<sup>[105]</sup> demonstrated a planar-nanostrip-channel GaN HEMT device to improve  $g_m$  and cut-off frequency. The gate on both sides of the fin are replaced by the partial arsenic ion implantation isolation in the channel region (see Fig. 17). It is found that the  $g_m$  of this device is wider over a large range of gate voltage, and the cut-off frequency is higher than nanowire structure as well because the gate-source parasitic capacitance is reduced. The aforementioned nanowire structures are proved to be useful for suppressing the increasing of  $r_s$  and the flatness of  $g_m$  of GaN HEMT is improved as a consequence.

#### 4.3. Graded channel

Previously, a kind of three-dimensional electron slab<sup>[106]</sup>, also called 3-D electron gas (3DEG) was realized by polarization bulk doping in the GaN HEMT to remove the scattering of ionized impurity and improve the electron mobility. The structure is shown in Fig. 18(a) and called polarization-graded

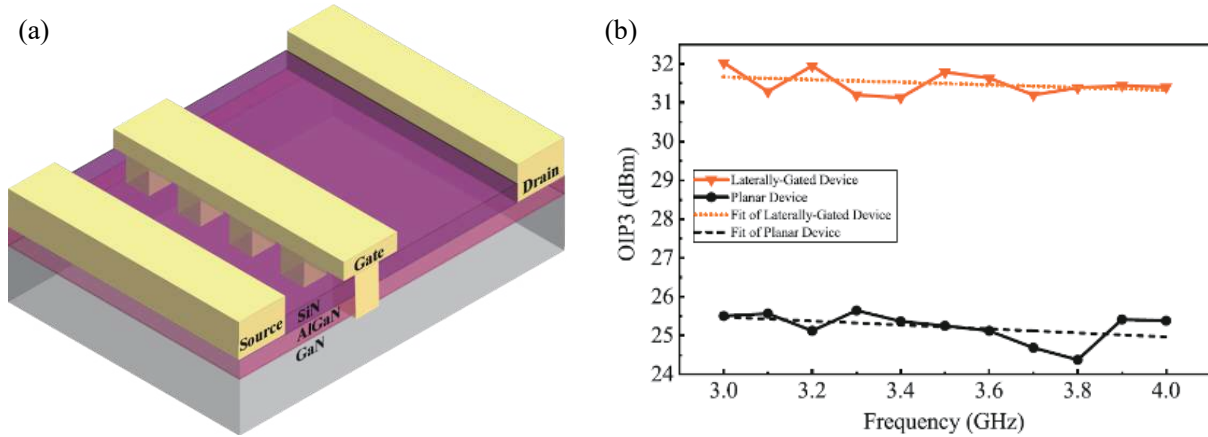


Fig. 15. (Color online) (a) Schematics of laterally gated device. (b) OIP3 of planar and laterally gated devices at 3–4 GHz range<sup>[102]</sup>.

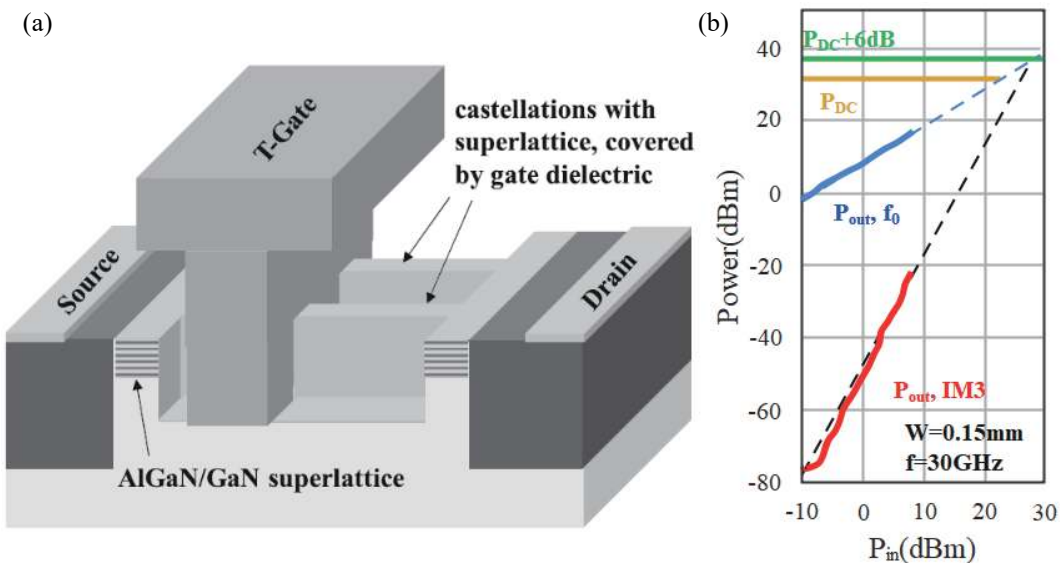


Fig. 16. (Color online) (a) Diagram of the super-lattice castellated FET structure combining a super-lattice epitaxial channel with a three-dimensional, castellated T-gate. (b) Two-tone linearity measurement at 30 GHz<sup>[103]</sup>.

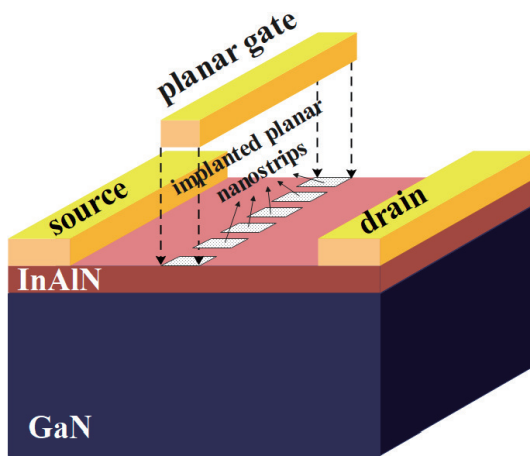


Fig. 17. (Color online) Schematic of planar nanostrip GaN HEMT<sup>[105]</sup>.

FET (PolFET). The channel is graded from GaN to  $\text{Al}_{0.35}\text{Ga}_{0.65}\text{N}$  to generate 3DEG. Fig. 18(b) depicts that, compared with the abrupt AlGaN/GaN structure, the energy band changes continuously from 20 to 40 nm, where the electrons distribute uniformly. The results turn out that the graded AlGaN/GaN structure has a wider GVS compared to conventional devices<sup>[107]</sup>. When the gate voltage increased, only the depletion width

decreases, but the volumetric charge density remains. In this way, the electron saturation velocity remains and the value of  $g_m$  is stable at a high gate voltage. Therefore, the PolFET achieves a flat  $g_m$  profile and a high device linearity<sup>[108, 109]</sup>.

Based on the graded channel, some novel structures are applied recently. Fang *et al.*<sup>[110]</sup> proposed an AlGaN/GaN HEMT with a step-graded layer that exhibits better linearity due to the individual optimization for each layer. Sohel *et al.*<sup>[111]</sup> reported an AlGaN/GaN HEMT with composite 2D and 3D electron channel (see Fig. 19(a)). The composite 2D-3D channel HEMT combines the advantages of 2DEG and 3DEG by offering high  $g_m$  and a tailored flat  $g_m$  profile. Fig. 19(b) shows an excellent OIP3/ $P_{DC}$  of 9.7 dB at 10 GHz. A device equipped with 50 nm T-gate length is proposed for mmWave application with 360 GHz  $f_{max}$  by Moon *et al.*<sup>[112]</sup>. This device has a flat  $g_m$  with a smaller  $g'_m$  and  $g''_m$ , which exhibits excellent linearity performance. Moon *et al.*<sup>[113]</sup> also reported a high-speed graded-channel GaN HEMT with 10 dB OIP3 improvement over the conventional AlGaN/GaN HEMT at the same DC power and demonstrated an OIP3/ $P_{DC}$  of 17–20 dB at 30 GHz. Hou *et al.*<sup>[114]</sup> proposed an AlGaN sandwich barrier (top AlGaN barrier, graded AlGaN barrier and bottom AlGaN barrier) HEMT with 3DEG to achieve high perfor-

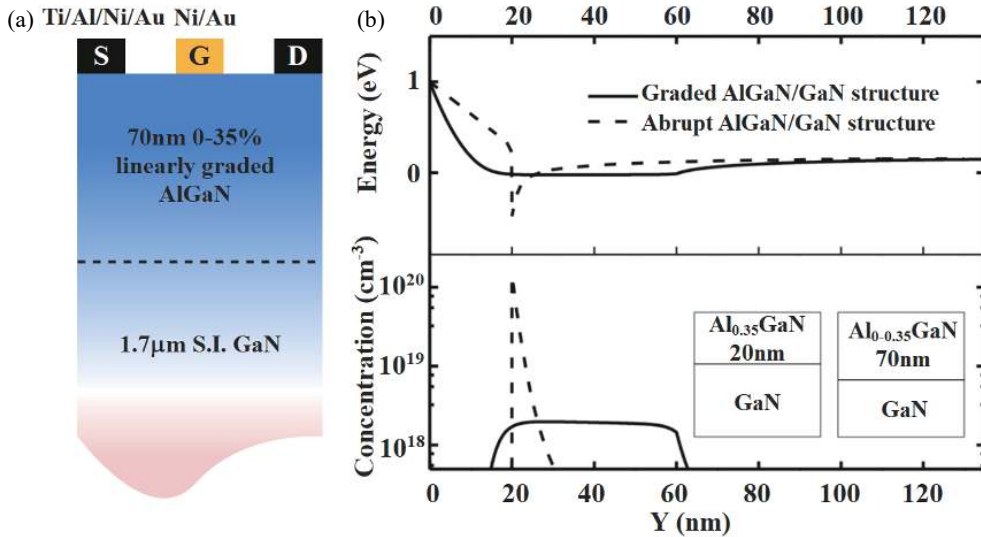


Fig. 18. (Color online) (a) Schematic cross section of AlGaN/GaN PolFET with graded heterostructure. (b) Top: energy-band profiles. Bottom: electron distributions. Inset: schematic cross section of PolFETs and HEMTs structures<sup>[107]</sup>.

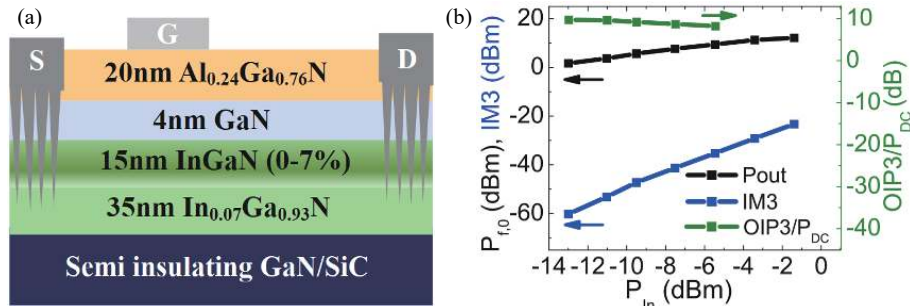


Fig. 19. (Color online) (a) Schematic diagram for the MOCVD-grown HEMT with a graded InGaN subchannel. (b) Two-tone linearity measurements with  $f_1 = 10$  GHz and  $f_2 = 10.01$  GHz biased near Class A<sup>[111]</sup>.

mance and linearity. Due to the sandwich barrier, the electric field peak can be suppressed effectively, which is helpful for the  $g_m$  flatness. According to the reports above, the graded channel with 3DEG is regarded as an effective way to reduce the scattering effects and improve the  $g_m$  flatness because of the wider electron distribution.

#### 4.4. Double channel

Although, the strong piezoelectric and spontaneous polarization result in a high concentration of 2DEG, they inevitably bring in a high perpendicular electric field that enhances scattering effects and dampens electron mobility<sup>[115]</sup>. Early, Liu *et al.*<sup>[116]</sup> reported a highly linear GaN HEMT with a composite-channel. Compared with the conventional HEMT, the channels consist of a major part formed by Al<sub>0.3</sub>Ga<sub>0.7</sub>N/Al<sub>0.05</sub>Ga<sub>0.95</sub>N hetero-interface and a minor part formed by Al<sub>0.05</sub>Ga<sub>0.95</sub>N/GaN hetero-interface. Due to the existence of a minor channel, on the one hand, the perpendicular electric field can be suppressed. On the other hand, the major and minor channels also pull the carrier distribution away from the barrier/channel interface and then the probability of scattering is reduced. As shown in Fig. 20, a GaN HEMT was fabricated on the epitaxial structure with a 1.5 nm AlN insertion layer to form a closely coupled double channel by Song *et al.*<sup>[117]</sup>. The balanced electron distribution between the upper and lower channels effectively alleviates the influence of the optical scattering under the high electric

field, which is useful for the  $g_m$  flatness. In a recent study, an AlGaN/GaN/graded-AlGaN:Si-doped/GaN double-channel HEMT is reported by Yu *et al.*<sup>[118]</sup>. Due to the Si-doped graded bottom barrier, the presented HEMT shows a broader and flatter  $g_m$  profile compared with the traditional double-channel HEMT. As a result, an OIP3 of 39.3 dBm is achieved at 3.6 GHz.

The suppression of increasing access resistance is the other profit of the double channel. At the high current level, carriers start to partially flow through the top channel and from this channel to the bottom channel by tunneling and other mechanisms, which is helpful for maintaining the access resistance<sup>[119]</sup>. Generally, the double channel is a good solution for the problems of scattering effect and access resistance increasing.

#### 4.5. Transconductance compensation

A novel device-level  $g_m$  compensation is also an effective way to improve device linearity. According to Joglekar *et al.*<sup>[30]</sup>, the core idea of the  $g_m$  compensation is that by connecting multiple FETs in parallel with different gate-overdrive quiescent bias voltages, the effective  $g_m$  derivatives of the FET in RF application can be reduced. In Fig. 21, by connecting multiple device elements with different threshold voltages, the  $g_m$  derivation is suppressed. Because of this, see Fig. 22, along with the width direction of the gate finger, many fins with different period widths ( $W$ ) are integrated together. As such, the value of  $g_m$  is compensated by these fins that are equipped

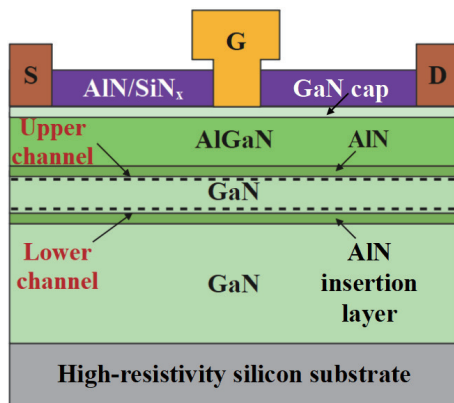


Fig. 20. (Color online) Cross-sectional schematic of the double-channel HEMT on the GaN on high-resistivity silicon<sup>[117]</sup>.

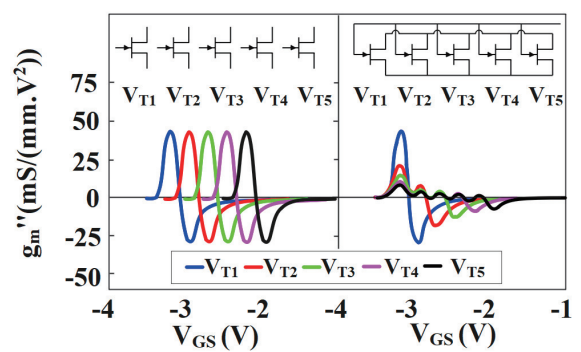


Fig. 21. (Color online) Illustration of device-level  $g_m$ -compensation- $g_m''$  for a set of five independent transistors with slight (0.2–0.3 V) offsets in threshold voltage (left). When these transistors are connected together (right), the composite  $g_m''$  (black curve) is lowered<sup>[30]</sup>.

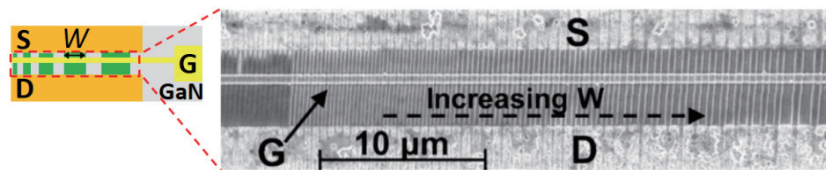


Fig. 22. (Color online) Schematic and SEM image of the fin device. The widths of the five fin devices are all present within the single fin device<sup>[30]</sup>.

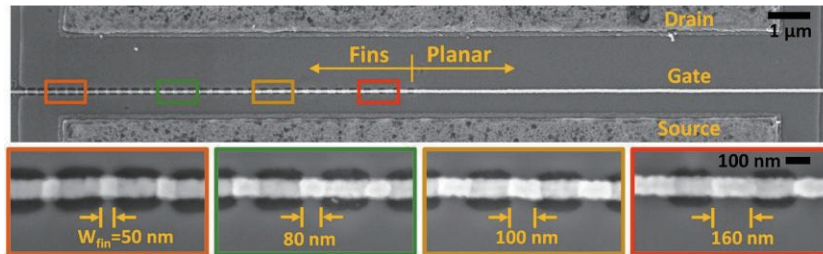


Fig. 23. (Color online) Top-view SEM images of the fabricated device showing a planar region and a fin region under a single gate electrode<sup>[120]</sup>.

with different threshold voltages. Subsequently, to overcome the shortage of the limited tunability range for threshold voltage, Choi *et al.*<sup>[120]</sup> synthesized the planar HEMT with the multiple narrow Fin-HEMT together (see Fig. 23). A highly linear  $g_m$  plateau of >6 V results in a record linearity figure of merit OIP3/P<sub>DC</sub> of 15.9 dB at 5 GHz.

Besides the Fin-HEMT used for the  $g_m$  compensation, many other structures are employed to realize this technique in recent studies. Wang *et al.*<sup>[121]</sup> proposed a Fin-like HEMT by utilizing the  $g_m$  compensation to achieve high linearity. They periodically etch the gate depth along the gate strip direction and two different threshold voltages are compensated each other. Finally, the device offers an exceptional linearity, in the form of a GVS of >5.6 V, a 17 dB improvement in IMD3 and a 7.5 dB improvement in OIP3 at 8 GHz. Similarly, Wu *et al.*<sup>[122]</sup> proposed a high linearity GaN HEMT with gradually changing gate recess etch along the gate strip (see Fig. 24). Due to the taper-etched AlGaN layer beneath the gate, the threshold voltage at different positions is different, which can be in the form of the  $g_m$  compensation. The device exhibits a high output current of 1.12 A/mm and a high peak extrinsic  $g_m$  of 374 mS/mm with an improved GVS of >2.6 V.

#### 4.6. Others

There are some applications of novel material and special structure are proposed to pursue a higher GVS. Gao *et al.*<sup>[123]</sup> employed the nonlinear ferroelectric material of

Pb(Zr<sub>0.52</sub>Ti<sub>0.48</sub>)O<sub>3</sub> (PZT) as the gate dielectric to enhance the linearity of the GaN HEMT. With the increasing gate voltage, the PZT goes into the nonlinear region and changes the concentration of 2DEG due to its nonlinear polarization effect. It is observed in Fig. 25 that an extra hump is induced, further making a large GVS of 4.3 V. Zhang *et al.*<sup>[124]</sup> inserted an InGaN channel between the AlGaN barrier and the GaN buffer layers to enhance the confinement of 2DEG and the good gate control capability. As a result, the  $g_m$  profile maintains stable without obvious degradation over the gate voltage ranging from -3.2 to -0.2 V. Similarly, compared with the Ga-polar, the N-polar hetero-structure has a strong back-barrier effect due to the absence of inversion symmetry in wurtzite III-nitride materials, which improves electron confinement<sup>[125]</sup>. Thus, the N-polar hetero-structure is useful for the  $g_m$  flatness and the improvement of the device linearity. Arias *et al.*<sup>[126]</sup> reported a N-polar GaN HEMT with OIP3/P<sub>DC</sub> of 12 dB at 10 GHz for high-performance X-band application. Guidry *et al.*<sup>[127]</sup> demonstrated a N-polar metal insulator semiconductor (MIS) HEMT with a deep recess gate having OIP3/P<sub>DC</sub> of 11.4 dB at 30 GHz. In addition, Shrestha *et al.*<sup>[128]</sup> proposed a N-polar GaN MIS-HEMT simultaneously to achieve a high linearity (OIP3/P<sub>DC</sub> of 15 dB) and a high gain (12.7 dB) at 30 GHz.

Some special structures were also proposed to improve the linearity of the device. Wang *et al.*<sup>[129]</sup> found the dual-gate structure is of benefit to the linearity improvement (see

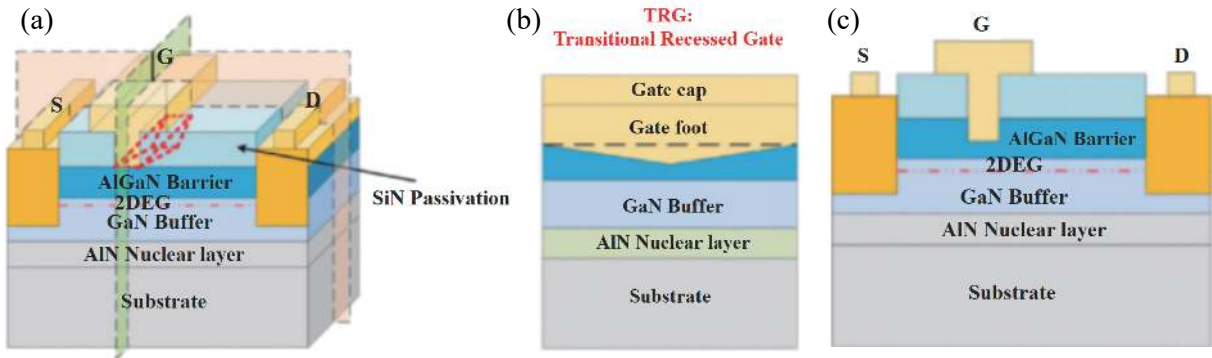


Fig. 24. (Color online) (a) TRG-HEMT structure diagram. (b) Cross section view of the TRG-HEMT along the gate width. (c) Cross section view of the TRG-HEMT along the gate length<sup>[122]</sup>.

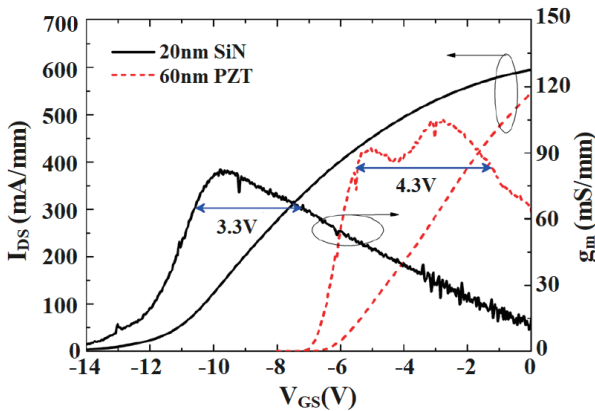


Fig. 25. (Color online) Transfer characteristics of the AlGaN/GaN MIS-HEMTs with 20 nm SiN and 60 nm PZT at  $V_{DS} = 10$  V<sup>[123]</sup>.

**Fig. 26.** With the help of the dual-gate structure, the electric field is alleviated by the second gate and the device exhibits a large GVS of 3.1 V. Two-tone measurement results show that, when measured at 6 GHz, the device has an OIP3 of 26.56 dBm and an OIP3/P<sub>DC</sub> ratio of 14.37 dB. Lenka *et al.*<sup>[130]</sup> combined the PZT material with the dual-gate structure to develop a dual-gate ferroelectric GaN HEMT (see Fig. 27). With the benefits of the dual gate and the PZT material, a larger GVS of 5.2 V and a good suppression of IMD3 around 10 dB are obtained.

#### 4.7. Discussions

Numerous novel structures and materials were applied on the GaN HEMT to improve the  $g_m$  flatness based on the mechanisms of nonlinear  $g_m$ . The GVS and peak  $g_m$  of the above-mentioned improvement methods are summarized in Fig. 28. It is noted that, most values of the GVS exceed 3 V and some of them are even greater than 6 V, such as the nanowire channel and the  $g_m$  compensation. It means that the value of  $g_m$  is stable over a wide gate voltage range and a high linearity of the GaN HEMT is guaranteed. However, most values of the peak  $g_m$  are nearly 100 to 200 mS/mm which are not high. Especially, the GaN HEMT with a large GVS is usually accompanied with a small peak  $g_m$ , which will influence the power gain of PAs. In this way, there is a risk that the power gain will be influenced by the small peak  $g_m$  when the GaN HEMT is used in the PAs<sup>[27]</sup>.

Fig. 29 shows the two-tone measurement results of these methods. Most of them have large values of OIP3 at the frequency from 1 GHz to 30 GHz. Considering the different mea-

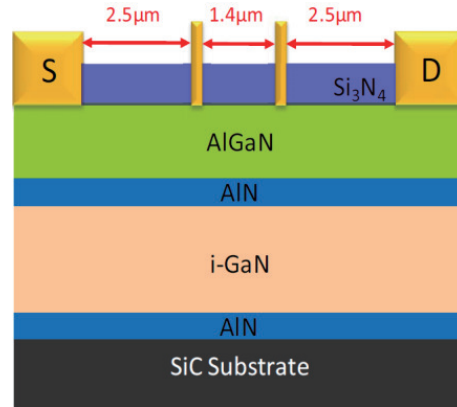


Fig. 26. (Color online) Schematic cross section of the AlGaN/GaN HEMT with a dual-gate structure<sup>[129]</sup>.

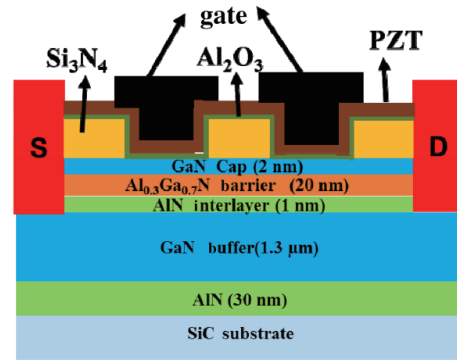


Fig. 27. (Color online) Cross-sectional view of dual gate ferroelectric GaN HEMT<sup>[130]</sup>.

surement frequencies and operation states, it is actually difficult to infer the best method or the worst one. To understand the distinctions further, we classify the mechanisms and the challenges of these methods in Table 1. The trapping suppression methods only focus on the trap-induced  $g_m$  reduction. Most of these methods seem to have no ability to further improve the GVS at present. Merely, the surface passivation cannot only eliminate the surface traps of the GaN HEMT, but also improve the  $g_m$  flatness by making use of the charge and electric field modulation. As for the nanowire channel structure, the channel region is partly etched to improve the current driving capability for the source access region and the results show an effective suppression of  $r_s$ . Even though, the extra parasitic gate capacitance is induced by the extra gate region beside both sides of the fins. Considering

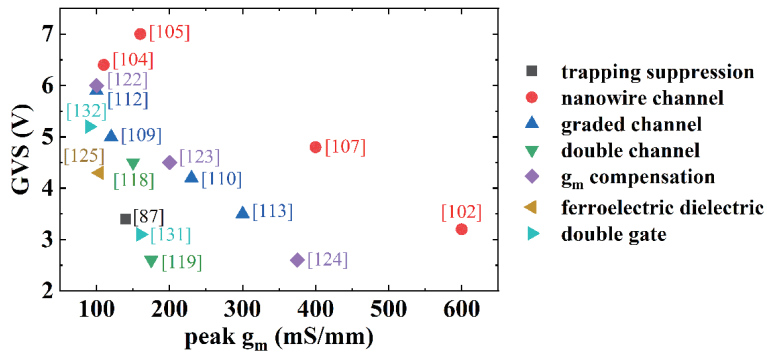
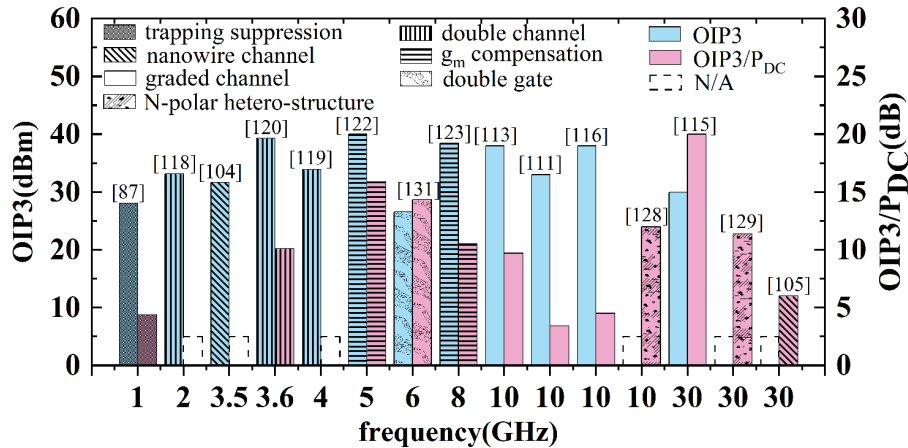
Fig. 28. (Color online) Reported GVS and peak  $g_m$  of recent improvement methods for the GaN HEMT.

Fig. 29. (Color online) Reported results of two-tone linearity measurement of recent improvement methods for the GaN HEMT.

Table 1. Features of reported improvement methods for nonlinear  $g_m$ .

Types	Mechanisms	Challenges
Trapping suppression	Reduce the electric field; eliminate the sources of the traps; keep the 2DEG from the traps	Mostly have no ability to further improve the GVS
Nanowire channel (fin structure/tri-gate)	Effectively suppress the increasing of $r_s$ due to the large current drivability	Extra parasitic gate capacitance; loss of the output current; etching damage risk
Graded channel (POLFET with 3DEG)	Maintain the stable electron volume to suppress scattering	Low peak $g_m$ ; complex epitaxy process of the graded channel
Double channel	Reduce perpendicular electric field; electron compensation between double channel	Multiple epitaxy of the double channel
$g_m$ compensation	Different $g_m$ compensated with each other	Precise design for threshold voltage; hard process control for stable threshold
Ferroelectric dielectric/N-polar hetero-structure	Nonlinear polarization effect of PZT / improvement of electron confinement	Tough epitaxy growth of N-polar
Double gate	Alleviate the electric field	Low peak $g_m$

the partial etching of the channel region, the output current is sacrificed by the etching region and the damage induced by etching needs to be concerned.

The graded channel with 3DEG is found to be expert in the suppression of  $g_m$  reduction with the benefit of its stable electron volume. However, the original 2DEG is forced to distribute as 3DEG, the value of peak  $g_m$  is reduced<sup>[108]</sup>. Also, the complex epitaxial structure of the graded channel will be an obstacle for massive applications. The GaN HEMT with a double channel can improve the  $g_m$  flatness resulting from the reduction of the perpendicular electric field and the electron compensation between the double channel. The multiple epitaxy needs to be carried out to form the double channel, unconsciously increasing the process complexity.

The  $g_m$  compensation can achieve the larger GVS by the well design. Its realization is diversity, including the fin structure with different period width, fin-like structure, taper-etched AlGaN layer. However, the threshold voltage of each element needs to be designed precisely to maintain an effective compensation. Therefore, the design difficulty is higher than other methods. It is necessary to guarantee a stable threshold voltage with the strict control of the fabrication process. The application of new material includes ferroelectric material and N-polar hetero-structure. Although these methods are effective for the device linearity, the side effects of the new material on device features are still unknown. For the N-polar GaN, it is difficult to achieve a smooth surface morphology when compared with the Ga-polar one<sup>[125, 131]</sup>. As

such, these may be the potential obstacles for these individual methods.

## 5. Summary

The increasing demands of communication require a high-performance wireless communication system. The GaN HEMT is the potential candidate for the RF front-end applications due to the high frequency and large power handling capability. High linearity is the key index to ensure the signal quality and the transmission rate. The circuit-level linearization techniques have been applied effectively. However, as the frequency increases to the mmWave range even more, the complexity and the cost of linearization are also increased at the circuit level. Thus, the device-level methods seem to be effective and low-cost. When the GaN HEMT used in the PAs, many factors can result in nonlinearity such as the parasitic capacitance, the nonlinear  $g_m$  profile, the leakage current and so on, wherein the nonlinear  $g_m$  is considered as the main contributor. The physical mechanisms of  $g_m$  reduction are attributed to the decrease of the electron mobility and velocity induced by the scattering in the high electric field or high concentration state, the increasing access resistance induced by the space charge limitation or high electric field, the self-heating effect and the trapping effects.

Besides the self-heating for which we can enhance heat dissipation at the package level or apply a substrate with high thermal conductivity, plenty of device-level improvement methods are proposed based on the physical mechanisms of nonlinear  $g_m$  in recent years. First of all, the trapping effects are the main sources for the nonlinear  $g_m$ . Many trapping suppression methods, including the surface passivation, the gate/source field plate, the GaN cap layer and some elaborated epitaxial structures, were demonstrated to be effective. However, the improvement effect is limited. In this way, other methods in the device epitaxial process and structure were proposed with better effects. The nanowire channel HEMT (Fin-HEMT/tri-gate HEMT) effectively suppresses the increasing  $r_s$ . The graded channel with 3DEG maintains the stable electron volume to prevent the scattering effect. The double-channel HEMT reduces the perpendicular electric field and  $r_s$ . The  $g_m$  compensation is an effective way of broadening GVS by integrating many device elements with different threshold voltage. The PZT material, N-polar hetero-structure and double gate are also employed to improve linearity. As we can see in Fig. 29, the different methods are verified under different frequencies ranging from 1 to 30 GHz. Therefore, we need to identify the suitable methods for different scenarios, especially, for the higher frequency and larger power applications in the RF front ends.

Moreover, the composite methods seem to be a trend for the linearity improvement, such as the above-mentioned combination of the double gate and the PZT, the composite channel of 2DEG and 3DEG, and the  $g_m$  compensation applied with fin structure. It is reasonably believed that the application of composite methods can provide the better effect for the device linearity by utilizing their composite advantages.

## Acknowledgements

This work was supported by the Shenzhen Science and Technology Program on Key Basic Research Project under

grant JCYJ20210324120409025 and the National Natural Science Foundation of China under grant 61904135.

## References

- [1] Jones E A, Wang F F, Costinett D. Review of commercial GaN power devices and GaN-based converter design challenges. *IEEE J Emerg Sel Top Power Electron*, 2016, 4, 707
- [2] Singh S, Chaudhary T, Khanna G. Recent advancements in wide band semiconductors (SiC and GaN) technology for future devices. *Silicon*, 2022, 14, 5793
- [3] Roccaforte F, Fiorenza P, Greco G, et al. Emerging trends in wide band gap semiconductors (SiC and GaN) technology for power devices. *Microelectron Eng*, 2018, 187/188, 66
- [4] Aubry R, Jacquet J C, Oualali M, et al. ICP-CVD SiN passivation for high-power RF InAlGaN/GaN/SiC HEMT. *IEEE Electron Device Lett*, 2016, 37, 629
- [5] Kumar V, Lu W, Schwindt R, et al. AlGaN/GaN HEMTs on SiC with  $f_T$  of over 120 GHz. *IEEE Electron Device Lett*, 2002, 23, 455
- [6] Zhang Y C, Wei K, Huang S, et al. High-temperature-recessed millimeter-wave AlGaN/GaN HEMTs with 42.8% power-added-efficiency at 35 GHz. *IEEE Electron Device Lett*, 2018, 39, 727
- [7] Du H H, Zhang J C, Zhou H, et al. GaN high-electron-mobility-transistor on free-standing GaN substrate with low contact resistance and state-of-the-art  $f_T \times L_G$  value. *IEEE Trans Electron Devices*, 2022, 69, 968
- [8] Micovic M, Brown D F, Regan D, et al. High frequency GaN HEMTs for RF MMIC applications. *2016 IEEE International Electron Devices Meeting (IEDM)*, 2016, 653
- [9] Tan J, Yuk K S, Branner G R. Design of a high power, wideband power amplifier using AlGaN/GaN HEMT. *2017 IEEE 18th Wireless and Microwave Technology Conference (WAMICON)*, 2017, 1
- [10] Joshi R, Liu M H, Hsu S S H. A high efficiency compact class F GaN MMIC power amplifier for 5G applications. *2020 50th European Microwave Conference (EuMC)*, 2021, 1103
- [11] Polli G, Del Gaudio A, De Padova A, et al. A high-performance C-band integrated front-end in AlGaN/GaN technology. *2018 International Workshop on Integrated Nonlinear Microwave and Millimetre-wave Circuits (INMMIC)*, Brive La Gaillarde, France, 2018, 1
- [12] Iuolano F, Boles T. GaN-on-Si HEMTs for wireless base stations. *Mater Sci Semicond Process*, 2019, 98, 100
- [13] Nunes L C, Cabral P M, Pedro J C. AM/AM and AM/PM distortion generation mechanisms in Si LDMOS and GaN HEMT based RF power amplifiers. *IEEE Trans Microw Theory Tech*, 2014, 62, 799
- [14] Cheaito A, Crussiere M, Louet Y, et al. EVM derivation for multi-carrier signals: Joint impact of non-linear amplification and pre-distortion. *2015 IEEE 81st Vehicular Technology Conference (VTC Spring)*, 2015, 1
- [15] Pedro J C, Nunes L C, Cabral P M. Soft compression and the origins of nonlinear behavior of GaN HEMTs. *2014 9th European Microwave Integrated Circuit Conference*, Rome, Italy, 2014, 1297
- [16] Kobayashi K W. Bias optimized IP2 & IP3 linearity and NF of a decade-bandwidth GaN MMIC feedback amplifier. *2012 IEEE Radio Frequency Integrated Circuits Symposium*, Montreal, QC, Canada, 2012, 479
- [17] Guan L, Zhu A D. Green communications: Digital predistortion for wideband RF power amplifiers. *IEEE Microw Mag*, 2014, 15(7), 84
- [18] Choi P, Radhakrishna U, Boon C C, et al. Linearity enhancement of a fully integrated 6-GHz GaN power amplifier. *IEEE Microw Wirel Compon Lett*, 2017, 27, 927
- [19] Ren J J. A new digital predistortion algorithms scheme of feed-back FIR cross-term memory polynomial model for short-wave

- power amplifier. *IEEE Access*, 2020, 8, 38327
- [20] Tomé P M, Barradas F M, Cunha T R, et al. Hybrid analog/digital linearization of GaN HEMT-based power amplifiers. *IEEE Trans Microw Theory Tech*, 2019, 67, 288
- [21] Abuelma'atti M T, Abuelmaatti A M T, Yeung T, et al. Linearization of GaN power amplifier using feedforward and predistortion techniques. *2011 3rd Asia Symposium on Quality Electronic Design (ASQED)*, Kuala Lumpur, Malaysia, 2011, 282
- [22] Moore K, Green B, Klingbeil S, et al. High performance 150 mm RF GaN technology with low memory effects. *2020 IEEE BiCMOS and Compound Semiconductor Integrated Circuits and Technology Symposium (BCICTS)*, Monterey, CA, USA, 2021, 1
- [23] Lin C K, Du J H, Wang A, et al. Pure-play GaN foundry technology for RF applications. *2014 Asia-Pacific Microwave Conference*, Sendai, Japan, 2015, 188
- [24] Nayak S, Kao M Y, Chen H T, et al. 0.15  $\mu\text{m}$  GaN MMIC manufacturing technology for 2-50 GHz power applications. *Conference on Compound Semiconductor Manufacturing Technology*, Scottsdale, Arizona, USA, 2015, 43
- [25] Nagy W, Brown J, Borges R, et al. Linearity characteristics of microwave-power GaN HEMTs. *IEEE Trans Microw Theory Tech*, 2003, 51, 660
- [26] Srinidhi E R, Kompa G. Investigation of IMD3 in GaN HEMT based on extended Volterra series analysis. *2007 European Microwave Integrated Circuit Conference*, Munich, Germany, 2007, 52
- [27] Ahmed A, Islam S S, Anwar A F M. A temperature-dependent nonlinear analysis of GaN/AlGaN HEMTs using Volterra series. *IEEE Trans Microw Theory Tech*, 2001, 49, 1518
- [28] Garcia J A, Sanchez A M, Pedro J C, et al. Characterizing the gate-to-source nonlinear capacitor role on GaAs FET IMD performance. *IEEE Trans Microw Theory Tech*, 1998, 46, 2344
- [29] Sarbishaei H, Wu D Y T, Boumaiza S. Linearity of GaN HEMT RF power amplifiers-a circuit perspective. *2012 IEEE/MTT-S International Microwave Symposium Digest*, Montreal, QC, Canada, 2012, 1
- [30] Joglekar S, Radhakrishna U, Piedra D, et al. Large signal linearity enhancement of AlGaN/GaN high electron mobility transistors by device-level  $V_t$  engineering for transconductance compensation. *2017 IEEE International Electron Devices Meeting (IEDM)*, San Francisco, CA, USA, 2018, 25.3.1
- [31] Maas S A. Nonlinear microwave and RF circuits. 2nd ed. Artech House, 1997
- [32] Tarakji A, Fatima H, Hu X, et al. Large-signal linearity in III-N MOSDHFETs. *IEEE Electron Device Lett*, 2003, 24, 369
- [33] Garcia J A, Aballo T, Mediavilla A, et al. Characterizing the  $I_{GS}(V_{GS})$  nonlinearity for describing its contribution to FET large-signal intermodulation distortion. *2006 International Workshop on Integrated Nonlinear Microwave and Millimeter-Wave Circuits*, Aveiro, Portugal, 2006, 80
- [34] Liu Z H, Ng G I, Arulkumaran S, et al. Improved linearity for low-noise applications in 0.25- $\mu\text{m}$  GaN MISHEMTs using ALD  $\text{Al}_2\text{O}_3$  as gate dielectric. *IEEE Electron Device Lett*, 2010, 31, 803
- [35] Oxley C H, Uren M J, Coates A, et al. On the temperature and carrier density dependence of electron saturation velocity in an AlGaN/GaN HEMT. *IEEE Trans Electron Devices*, 2006, 53, 565
- [36] Ridley B K, Schaff W J, Eastman L F. Hot-phonon-induced velocity saturation in GaN. *J Appl Phys*, 2004, 96, 1499
- [37] Fang T, Wang R H, Xing H L, et al. Effect of optical phonon scattering on the performance of GaN transistors. *IEEE Electron Device Lett*, 2012, 33, 709
- [38] Bajaj S, Shoron O F, Park P S, et al. Density-dependent electron transport and precise modeling of GaN high electron mobility transistors. *Appl Phys Lett*, 2015, 107, 153504
- [39] Juang J R, Huang T Y, Chen T M, et al. Transport in a gated  $\text{Al}_{0.18}\text{Ga}_{0.82}\text{N}/\text{GaN}$  electron system. *J Appl Phys*, 2003, 94, 3181
- [40] Li T, Joshi R P, Fazi C. Monte Carlo evaluations of degeneracy and interface roughness effects on electron transport in AlGaN-GaN heterostructures. *J Appl Phys*, 2000, 88, 829
- [41] Palacios T, Rajan S, Chakraborty A, et al. Influence of the dynamic access resistance in the g/sub m/ and f/sub T/ linearity of AlGaN/GaN HEMTs. *IEEE Trans Electron Devices*, 2005, 52, 2117
- [42] Tirado J M, Mieville F, Zhao X, et al. Origin of the increasing access resistance in AlGaN/GaN HEMTs. *2008 Device Research Conference*, Santa Barbara, CA, USA, 2008, 203
- [43] Wu Y R, Singh M, Singh J. Sources of transconductance collapse in III-V nitrides-consequences of velocity-field relations and source/gate design. *IEEE Trans Electron Devices*, 2005, 52, 1048
- [44] Trew R J, Liu Y Y, Bilbro L, et al. Nonlinear source resistance in high-voltage microwave AlGaN/GaN HFETs. *IEEE Trans Microw Theory Tech*, 2006, 54, 2061
- [45] Yang M, Lin Z J, Zhao J T, et al. Effect of polarization coulomb field scattering on parasitic source access resistance and extrinsic transconductance in AlGaN/GaN heterostructure FETs. *IEEE Trans Electron Devices*, 2016, 63, 1471
- [46] Chen C H, Sadler R, Wang D, et al. The causes of GaN HEMT bell-shaped transconductance degradation. *Solid State Electron*, 2016, 126, 115
- [47] Kuzmik J, Javorka R, Alam A, et al. Determination of channel temperature in AlGaN/GaN HEMTs grown on sapphire and silicon substrates using DC characterization method. *IEEE Trans Electron Devices*, 2002, 49, 1496
- [48] Mitrofanov O, Manfra M. Mechanisms of gate lag in GaN/AlGaN/GaN high electron mobility transistors. *Superlattices Microstruct*, 2003, 34, 33
- [49] Tirado J M, Sanchez-Rojas J L, Izpura J I. Trapping effects in the transient response of AlGaN/GaN HEMT devices. *IEEE Trans Electron Devices*, 2007, 54, 410
- [50] Hu W D, Chen X S, Lu W. Intrinsic mechanism of drain-lag and current collapse in GaN-based HEMTs. *2009 IEEE Workshop on Microelectronics and Electron Devices*, Boise, ID, USA, 2009, 1
- [51] Binari S C, Ikossi K, Roussos J A, et al. Trapping effects and microwave power performance in AlGaN/GaN HEMTs. *IEEE Trans Electron Devices*, 2001, 48, 465
- [52] Meneghesso G, Verzellesi G, Pierobon R, et al. Surface-related drain current dispersion effects in AlGaN-GaN HEMTs. *IEEE Trans Electron Devices*, 2004, 51, 1554
- [53] Mollah S, Gaevski M, Hussain K, et al. Current collapse in high-Al channel AlGaN HFETs. *Appl Phys Express*, 2019, 12, 074001
- [54] Tirado J M, Sanchez-Rojas J L, Izpura J I. Simulation of surface state effects in the transient response of AlGaN/GaN HEMT and GaN MESFET devices. *Semicond Sci Technol*, 2006, 21, 1150
- [55] Meneghini M, Ronchi N, Stocco A, et al. Investigation of trapping and hot-electron effects in GaN HEMTs by means of a combined electrooptical method. *IEEE Trans Electron Devices*, 2011, 58, 2996
- [56] Vetry R, Zhang N Q, Keller S, et al. The impact of surface states on the DC and RF characteristics of AlGaN/GaN HFETs. *IEEE Trans Electron Devices*, 2001, 48, 560
- [57] Saito Y, Tsurumaki R, Noda N, et al. Analysis of reduction in lag phenomena and current collapse in field-plate AlGaN/GaN HEMTs with high acceptor density in a buffer layer. *IEEE Trans Device Mater Reliab*, 2018, 18(1), 46
- [58] Meneghesso G, Meneghini M, Bisi D, et al. Trapping phenomena in AlGaN/GaN HEMTs: A study based on pulsed and transient measurements. *Semicond Sci Technol*, 2013, 28, 074021
- [59] Du J F, Chen N T, Jiang Z G, et al. Study on transconductance non-linearity of AlGaN/GaN HEMTs considering acceptor-like traps in barrier layer under the gate. *Solid State Electron*, 2016, 115, 60
- [60] Binari S C, Klein P B, Kazior T E. Trapping effects in GaN and SiC microwave FETs. *Proc IEEE*, 2002, 90, 1048

- [61] Kohn E, Daumiller I, Schmid P, et al. Large signal frequency dispersion of AlGaN/GaN heterostructure field effect transistors. *Electron Lett*, 1999, **35**, 1022
- [62] Xie S X, Paidi V, Heikman S, et al. High linearity GaN HEMT power amplifier with pre-linearization gate diode. *IEEE Lester Eastman Conference on High Performance Devices*, Troy, NY, USA, 2004, 223
- [63] Bothe K M, Ganguly S, Guo J, et al. Improved X-band performance and reliability of a GaN HEMT with Sunken source connected field plate design. *IEEE Electron Device Lett*, 2022, **43**, 354
- [64] Wu Y F, Saxler A, Moore M, et al. 30-W/mm GaN HEMTs by field plate optimization. *IEEE Electron Device Lett*, 2004, **25**, 117
- [65] Brown D F, Tang Y, Regan D A, et al. Self-aligned AlGaN/GaN FinFETs. *IEEE Electron Device Lett*, 2017, **38**, 1445
- [66] Zhang J Q, Wang L, Li L A, et al. Self-aligned-gate AlGaN/GaN heterostructure field-effect transistor with titanium nitride gate. *Chin Phys B*, 2016, **25**, 087308
- [67] Khalil I, Bahat-Treidel E, Schnieder F, et al. Improving the linearity of GaN HEMTs by optimizing epitaxial structure. *IEEE Trans Electron Devices*, 2009, **56**, 361
- [68] Aggarwal R, Agrawal A, Gupta M, et al. Improved linearity performance of AlGaN/GaN MISFET over conventional HFETs: An optimization study for wireless infrastructure applications. *Superlattices Microstruct*, 2011, **50**, 1
- [69] Hasan M T, Asano T, Tokuda H, et al. Current collapse suppression by gate field-plate in AlGaN/GaN HEMTs. *IEEE Electron Device Lett*, 2013, **34**, 1379
- [70] Suemitsu T, Kobayashi K, Hatakeyama S, et al. A new process approach for slant field plates in GaN-based high-electron-mobility transistors. *Jpn J Appl Phys*, 2016, **55**, 01AD02
- [71] Shao J H, Deng J N, Lu W, et al. Nanofabrication of 80 nm asymmetric T shape gates for GaN HEMTs. *Microelectron Eng*, 2018, **189**, 6
- [72] Arulkumaran S, Egawa T, Ishikawa H, et al. Surface passivation effects on AlGaN/GaN high-electron-mobility transistors with SiO<sub>2</sub>, Si<sub>3</sub>N<sub>4</sub>, and silicon oxynitride. *Appl Phys Lett*, 2004, **84**, 613
- [73] Vertiatchikh A V, Eastman L F, Schaff W J, et al. Effect of surface passivation of AlGaN/GaN heterostructure field-effect transistor. *Electron Lett*, 2002, **38**, 388
- [74] Bernát J, Javorka P, Fox A, et al. Effect of surface passivation on performance of AlGaN/GaN/Si HEMTs. *Solid State Electron*, 2003, **47**, 2097
- [75] Luo B, Johnson J W, Kim J, et al. Influence of MgO and Sc<sub>2</sub>O<sub>3</sub> passivation on AlGaN/GaN high-electron-mobility transistors. *Appl Phys Lett*, 2002, **80**, 1661
- [76] Gila B P, Thaler G T, Onstine A H, et al. New dielectrics for gate oxides and surface passivation on GaN. *2005 International Semiconductor Device Research Symposium*, Bethesda, MD, USA, 2005, 130
- [77] Joglekar S, Azize M, Jones E J, et al. Impact of Al<sub>2</sub>O<sub>3</sub> passivation on AlGaN/GaN nanoribbon high-electron-mobility transistors. *IEEE Trans Electron Devices*, 2016, **63**, 318
- [78] Koehler A D, Nepal N, Anderson T J, et al. Atomic layer epitaxy AlN for enhanced AlGaN/GaN HEMT passivation. *IEEE Electron Device Lett*, 2013, **34**, 1115
- [79] Oh M, Yang J W, Kim H, et al. Electrical characteristics of AlGaN/GaN high-electron-mobility transistors fabricated with a MgF<sub>2</sub> passivation layer. *J Korean Phys Soc*, 2020, **76**, 278
- [80] Lin Y S, Lin S F, Hsu W C. Microwave and power characteristics of AlGaN/GaN/Si high-electron mobility transistors with HfO<sub>2</sub> and TiO<sub>2</sub> passivation. *Semicond Sci Technol*, 2015, **30**, 015016
- [81] Green B M, Chu K K, Chumbes E M, et al. The effect of surface passivation on the microwave characteristics of undoped AlGaN/GaN HEMTs. *IEEE Electron Device Lett*, 2000, **21**, 268
- [82] Ansell B J, Harrison I, Foxon C T. The effect of surface passivation and illumination on the device properties of AlGaN/GaN HFETs. *Phys Stat Sol (a)*, 2001, **188**, 279
- [83] Lu W, Kumar V, Schwindt R, et al. A comparative study of surface passivation on AlGaN/GaN HEMTs. *Solid State Electron*, 2002, **46**, 1441
- [84] Liu J L, Mi M H, Zhu J J, et al. Improved power performance and the mechanism of AlGaN/GaN HEMTs using Si-rich SiN/Si<sub>3</sub>N<sub>4</sub> bilayer passivation. *IEEE Trans Electron Devices*, 2022, **69**, 631
- [85] Jing G J, Wang X H, Huang S, et al. Mechanism of linearity improvement in GaN HEMTs by low pressure chemical vapor deposition-SiN<sub>x</sub> passivation. *IEEE Trans Electron Devices*, 2022, **69**, 6610
- [86] Kordoš P, Bernát J, Marso M. Impact of layer structure on performance of unpassivated AlGaN/GaN HEMT. *Microelectron J*, 2005, **36**, 438
- [87] Meneghesso G, Rampazzo F, Kordos P, et al. Current collapse and high-electric-field reliability of unpassivated GaN/AlGaN/GaN HEMTs. *IEEE Trans Electron Devices*, 2006, **53**, 2932
- [88] Kikkawa T, Nagahara M, Okamoto N, et al. Surface-charge controlled AlGaN/GaN-power HFET without current collapse and gm dispersion. *International Electron Devices Meeting. Technical Digest (Cat. No.01CH37224)*, Washington, DC, USA, 2001, 25.4.1
- [89] Mitrofanov O, Manfra M, Weimann N. Impact of Si doping on radio frequency dispersion in unpassivated GaN/AlGaN/GaN high-electron-mobility transistors grown by plasma-assisted molecular-beam epitaxy. *Appl Phys Lett*, 2003, **82**, 4361
- [90] Uren M J, Moreke J, Kuball M. Buffer design to minimize current collapse in GaN/AlGaN HFETs. *IEEE Trans Electron Devices*, 2012, **59**, 3327
- [91] Chen D Y, Malmros A, Thorsell M, et al. Microwave performance of 'buffer-free' GaN-on-SiC high electron mobility transistors. *IEEE Electron Device Lett*, 2020, **41**, 828
- [92] Yao Y X, Huang S, Jiang Q M, et al. Identification of semi-ON-state current collapse in AlGaN/GaN HEMTs by drain current deep level transient spectroscopy. *IEEE Electron Device Lett*, 2022, **43**, 200
- [93] Kumazaki Y, Ohki T, Kotani J, et al. Over 80% power-added-efficiency GaN high-electron-mobility transistors on free-standing GaN substrates. *Appl Phys Express*, 2021, **14**, 016502
- [94] Ye R, Cai X L, Du C L, et al. An overview on analyses and suppression methods of trapping effects in AlGaN/GaN HEMTs. *IEEE Access*, 2022, **10**, 21759
- [95] Lee D S, Wang H, Hsu A, et al. Nanowire channel InAlN/GaN HEMTs with high linearity of g<sub>m</sub> and f<sub>T</sub>. *IEEE Electron Device Lett*, 2013, **34**, 969
- [96] Hisamoto D, Lee W C, Kedzierski J, et al. FinFET-a self-aligned double-gate MOSFET scalable to 20 nm. *IEEE Trans Electron Devices*, 2000, **47**, 2320
- [97] Zhang Y H, Zubair A, Liu Z H, et al. GaN FinFETs and trigate devices for power and RF applications: Review and perspective. *Semicond Sci Technol*, 2021, **36**, 054001
- [98] Lu B, Matioli E, Palacios T. Tri-gate normally-off GaN power MISFET. *IEEE Electron Device Lett*, 2012, **33**, 360
- [99] Zhang M, Ma X H, Yang L, et al. Influence of fin configuration on the characteristics of AlGaN/GaN fin-HEMTs. *IEEE Trans Electron Devices*, 2018, **65**, 1745
- [100] Zhang K, Kong Y C, Zhu G R, et al. High-linearity AlGaN/GaN FinFETs for microwave power applications. *IEEE Electron Device Lett*, 2017, **38**, 615
- [101] Shinohara K, King C, Carter A D, et al. GaN-based field-effect transistors with laterally gated two-dimensional electron gas. *IEEE Electron Device Lett*, 2018, **39**, 417
- [102] Odabaşı O, Yılmaz D, Aras E, et al. AlGaN/GaN-based laterally gated high-electron-mobility transistors with optimized linearity. *IEEE Trans Electron Devices*, 2021, **68**, 1016
- [103] Chang J, Afroz S, Nagamatsu K, et al. The super-lattice castel-

- lated field-effect transistor: A high-power, high-performance RF amplifier. *IEEE Electron Device Lett.*, 2019, 40, 1048
- [104] Shinohara K, King C, Regan E J, et al. GaN-based multi-channel transistors with lateral gate for linear and efficient millimeter-wave power amplifiers. *2019 IEEE MTT-S International Microwave Symposium (IMS)*, Boston, MA, USA, 2019, 1133
- [105] Xing W C, Liu Z H, Qiu H D, et al. Planar-nanostrip-channel In-AlN/GaN HEMTs on Si with improved  $g_m$  and  $f_T$  linearity. *IEEE Electron Device Lett.*, 2017, 38, 619
- [106] Jena D, Heikman S, Green D, et al. Realization of wide electron slabs by polarization bulk doping in graded III-V nitride semiconductor alloys. *Appl Phys Lett.*, 2002, 81, 4395
- [107] Fang Y L, Feng Z H, Yin J Y, et al. AlGaN/GaN polarization-doped field-effect transistors with graded heterostructure. *IEEE Trans Electron Devices*, 2014, 61, 4084
- [108] Bajaj S, Yang Z C, Akyol F, et al. Graded AlGaN channel transistors for improved current and power gain linearity. *IEEE Trans Electron Devices*, 2017, 64, 3114
- [109] Sohel S H, Xie A, Beam E, et al. X-band power and linearity performance of compositionally graded AlGaN channel transistors. *IEEE Electron Device Lett.*, 2018, 39, 1884
- [110] Fang Y L, Song X B, Feng Z H, et al. High linearity step-graded AlGaN/GaN heterojunction field effect transistor. *2016 13th China International Forum on Solid State Lighting: International Forum on Wide Bandgap Semiconductors China (SSLChina: IFWS)*, Beijing, China, 2016, 104
- [111] Sohel S H, Xie A, Beam E, et al. Polarization engineering of AlGaN/GaN HEMT with graded InGaN sub-channel for high-linearity X-band applications. *IEEE Electron Device Lett.*, 2019, 40, 522
- [112] Moon J S, Wong J, Grabar B, et al. 360 GHz fMAX graded-channel AlGaN/GaN HEMTs for mmW low-noise applications. *IEEE Electron Device Lett.*, 2020, 41, 1173
- [113] Moon J S, Grabar B, Antcliffe M, et al. High-speed graded-channel GaN HEMTs with linearity and efficiency. *2020 IEEE/MTT-S International Microwave Symposium (IMS)*, Los Angeles, CA, USA, 2020, 573
- [114] Hou B, Yang L, Mi M H, et al. High linearity and high power performance with barrier layer of sandwich structure and  $\text{Al}_{0.05}\text{GaN}$  back barrier for X-band application. *J Phys D: Appl Phys*, 2020, 53, 145102
- [115] Liu J, Zhou Y G, Chu R M, et al.  $\text{Al}_{0.3}\text{Ga}_{0.7}\text{N}/\text{Al}_{0.05}\text{Ga}_{0.95}\text{N}/\text{GaN}$  composite-channel HEMTs with enhanced linearity. *IEDM Technical Digest. IEEE International Electron Devices Meeting*, San Francisco, CA, USA, 2004, 811
- [116] Liu J E, Zhou Y G, Chu R M, et al. Highly linear  $\text{Al}_{0.3}\text{Ga}_{0.7}\text{N}-\text{Al}_{0.05}\text{Ga}_{0.95}\text{N}$ -GaN composite-channel HEMTs. *IEEE Electron Device Lett.*, 2005, 26, 145
- [117] Song W J, Zheng Z Y, Chen T, et al. RF linearity enhancement of GaN-on-Si HEMTs with a closely coupled double-channel structure. *IEEE Electron Device Lett.*, 2021, 42, 1116
- [118] Yu Q, Shi C Z, Yang L, et al. High current and linearity AlGaN/GaN-/graded-AlGaN: Si-doped/GaN heterostructure for low voltage power amplifier application. *IEEE Electron Device Lett.*, 2023, 44, 582
- [119] Palacios T, Chini A, Buttari D, et al. Use of double-channel heterostructures to improve the access resistance and linearity in GaN-based HEMTs. *IEEE Trans Electron Devices*, 2006, 53, 562
- [120] Choi W, Chen R J, Levy C, et al. Intrinsically linear transistor for millimeter-wave low noise amplifiers. *Nano Lett.*, 2020, 20, 2812
- [121] Wang P F, Ma X H, Mi M H, et al. Influence of fin-like configuration parameters on the linearity of AlGaN/GaN HEMTs. *IEEE Trans Electron Devices*, 2021, 68, 1563
- [122] Wu S, Ma X H, Yang L, et al. A millimeter-wave AlGaN/GaN HEMT fabricated with transitional-recessed-gate technology for high-gain and high-linearity applications. *IEEE Electron Device Lett.*, 2019, 40, 846
- [123] Gao T, Xu R M, Kong Y C, et al. Improved linearity in AlGaN/GaN metal-insulator-semiconductor high electron mobility transistors with nonlinear polarization dielectric. *Appl Phys Lett.*, 2015, 106, 243501
- [124] Zhang Y C, Zhang T, Zhou H, et al. InGaN-channel high-electron-mobility transistor with enhanced linearity and high-temperature performance. *Appl Phys Express*, 2018, 11, 094101
- [125] Wong M H, Keller S, Dasgupta N S, et al. N-polar GaN epitaxy and high electron mobility transistors. *Semicond Sci Technol*, 2013, 28, 074009
- [126] Arias A, Rowell P, Bergman J, et al. High performance N-polar GaN HEMTs with OIP<sub>3</sub>/Pdc ~12dB at 10GHz. *2017 IEEE Compound Semiconductor Integrated Circuit Symposium (CSICS)*, Miami, FL, USA, 2017, 1
- [127] Guidry M, Romanczyk B, Li H, et al. Demonstration of 30 GHz OIP<sub>3</sub>/PDC > 10 dB by mm-wave N-polar deep recess MISHEMTs. *2019 14th European Microwave Integrated Circuits Conference (EuMIC)*, Paris, France, 2019, 64
- [128] Shrestha P, Guidry M, Romanczyk B, et al. High linearity and high gain performance of N-polar GaN MIS-HEMT at 30 GHz. *IEEE Electron Device Lett.*, 2020, 41, 681
- [129] Wang H C, Su H F, Luc Q H, et al. Improved linearity in AlGaN/GaN HEMTs for millimeter-wave applications by using dual-gate fabrication. *ECS J Solid State Sci Technol*, 2017, 6, S3106
- [130] Panda D K, Lenka T R. Linearity improvement in E-mode ferroelectric GaN MOS-HEMT using dual gate technology. *Micro Nano Lett.*, 2019, 14, 618
- [131] Fichtenbaum N A, Schaake C, Mates T E, et al. Electrical characterization of p-type N-polar and Ga-polar GaN grown by metal-organic chemical vapor deposition. *Appl Phys Lett.*, 2007, 91, 172105



**Chenglin Du** received BS and PhD degrees from Nankai University, China, in 2014 and 2019 respectively. He is a member of the State Key Laboratory of Mobile Network and Mobile Multimedia Technology, ZTE corporation. His research focuses on radio-frequency GaN HEMTs.



**Ran Ye** received BS, MS and PhD degrees from Southeast University, China, in 2013, 2016 and 2020 respectively. He is a member of the State Key Laboratory of Mobile Network and Mobile Multimedia Technology, ZTE corporation. His research focuses on the reliability of semiconductor devices and radio-frequency GaN HEMTs.



**Xiaolong Cai** received BS and MS degrees from Jiangnan University, China, in 2012 and 2015, and a PhD degree from Nanjing University, China, in 2018. He is a member of the State Key Laboratory of Mobile Network and Mobile Multimedia Technology, ZTE corporation. His research includes the SiC optoelectronic device and radio-frequency GaN HEMTs.